

A KERNEL-BASED VIEW OF LANGUAGE MODEL FINE-TUNING

Sadhika Malladi, Alexander Wettig, Dingli Yu, Danqi Chen & Sanjeev Arora

Princeton University

{smalladi, awettig, dingliy, danqic, arora}@cs.princeton.edu

ABSTRACT

It has become standard to solve NLP tasks by fine-tuning pre-trained language models (LMs), especially in low-data settings. There is minimal theoretical understanding of empirical success, e.g., why fine-tuning a model with 10^8 or more parameters on a couple dozen training points does not result in overfitting. We investigate whether the Neural Tangent Kernel (NTK)—which originated as a model to study the gradient descent dynamics of infinitely wide networks with suitable random initialization—*describes* fine-tuning of pre-trained LMs. This study was inspired by the decent performance of NTK for computer vision tasks (Wei et al., 2022). We also extend the NTK formalism to fine-tuning with Adam. We present extensive experiments that show that once the downstream task is formulated as a language modeling problem through prompting, the NTK lens can often reasonably describe the model updates during fine-tuning with both SGD and Adam. This kernel view also suggests an explanation for success of parameter-efficient subspace-based fine-tuning methods. Finally, we suggest a path toward a formal explanation for our findings via Tensor Programs (Yang, 2020b).¹

1 INTRODUCTION

It is now customary to solve most supervised natural language processing (NLP) tasks such as topic classification and textual entailment by fine-tuning a pre-trained language model (e.g., Devlin et al. (2019); Liu et al. (2020b); Clark et al. (2020); Raffel et al. (2020); Joshi et al. (2020)). We lack theoretical understanding of this fine-tuning paradigm. Why do we not see over-fitting when fine-tuning a very large language model using a couple dozen instances of the supervised task? Why is fine-tuning so sensitive to details such as whether or not we include a prompt (e.g., adding “It was [great/terrible]” for sentiment analysis (Schick & Schütze, 2021; Gao et al., 2021)? Why does restricting optimization to a low-rank subspace of model parameters (Hu et al., 2021; Li et al., 2018; Aghajanyan et al., 2021) still result in performance comparable to full fine-tuning? Answering such questions requires understanding how the sequence of parameter updates changes in various scenarios, e.g., the addition of a prompt, or the introduction of randomly initialized parameters. The current theory of deep learning, at first sight, seems too primitive to address such questions, especially since fine-tuning has to start from a parameter initialization inherited from pre-training.

Recently, Wei et al. (2022) suggested replacing fine-tuning with Neural Tangent Kernel (NTK), an idea invented for study of infinite-width deep neural networks (Jacot et al., 2018; Du et al., 2019a) and previously applied to solving vision tasks with infinitely wide ConvNets (Arora et al. (2019b)). They note that NTK can be defined for any neural model f and any initialization θ_0 by representing an input ξ by the gradient it induces $\nabla f(\xi; \theta_0)$, which yields a kernel matrix:

$$\mathcal{K}(\xi, \xi') = \langle \nabla f(\xi; \theta_0), \nabla f(\xi'; \theta_0) \rangle. \quad (1)$$

This kernel is well-defined for any parameter vector θ_0 . However, for an infinite-width network initialized with θ_0 sampled from a suitably-scaled Gaussians, it can be shown that the kernel matrix is unchanged during gradient descent, which turns the classification task into a form of kernel regression with respect to this kernel (Jacot et al., 2018). In the fine-tuning setting, however, the initialization θ_0 is inherited from the pre-trained network, and not sampled from the Gaussian

¹Our code and pre-computed kernels are publicly available at github.com/princeton-nlp/LM-Kernel-FT.

distribution. Nevertheless, Wei et al. (2022) found that kernel regression using this “empirical NTK” (eNTK) defined with the inherited θ_0 performs well, achieving classification accuracy within 6% absolute of actual fine tuning on several image recognition tasks. In other words, their work hints that mathematical understanding of the fine-tuning phenomenon (e.g., its sample efficiency) could go via the theory of kernel classifiers.

The current paper furthers an empirical and theoretical understanding of the pre-training (PT) and fine-tuning (FT) paradigm for NLP tasks. We attempt to answer the following questions:

- *Does the eNTK method directly work for NLP tasks?* In Section 5, we show that eNTK does not work well for standard FT but it achieves performance comparable to prompt-based FT (Schick & Schütze, 2021; Gao et al., 2021) on a majority of downstream tasks that we evaluate.
- The NTK theory was developed for gradient descent, whereas LM fine-tuning often uses Adam (Kingma & Ba, 2015) as a standard practice (Devlin et al., 2019). *Can the above method be extended to give insight into the effect of different optimization algorithms?* In Section 4, we derive a new asymmetric “kernel” formula (Definition 4.2) that describes the dynamics of short-term training with Adam and shows that the corresponding eNTK achieves comparable performance as FT using Adam (Table 1).
- *Is the eNTK regression method simply an alternate model that also happens to have good performance on the classification task, or is it actually a near-equivalent description of how parameters of the original model evolve during fine-tuning?* Section 5.3 shows that for tasks that the eNTK can solve, the fine-tuning of the pre-trained model does exhibit behavior consistent with the dynamics of training kernel classifiers. See Definition 3.1.
- *If the eNTK can solve NLP tasks, then does the eNTK give insight into phenomena such as why prompting can improve performance and how parameter-efficient fine-tuning methods affect optimization?* Figure 1 demonstrates that adding a prompt is necessary for the eNTK to solve the task, and in Section 6, we apply the kernel lens to provide a possible explanation for the empirical success of subspace-based fine-tuning methods (Hu et al., 2021; Aghajanyan et al., 2021).

We conclude by proposing a rigorous mechanism through which fine-tuning of complex architectures (e.g., Transformers (Vaswani et al., 2017)) with prompts can exhibit kernel behavior. This is done in context of networks whose width goes to infinity, but unlike standard infinite-width NTK theory it allows a non-random initialization that is the result of pretraining. This result uses the Tensor Programs framework (Yang, 2019; 2020a;b; Yang & Littwin, 2021; Yang & Hu, 2021).

2 RELATED WORK

Kernel view of training. The infinite-width limit is a well-studied theoretical model for deep network optimization. Jacot et al. (2018) introduced NTK to capture training a deep and infinitely wide neural network from a random initialization. Subsequent experiments showed that the kernels underperformed for standard tasks (Arora et al., 2019b) but performed well on small datasets (i.e., hundreds of examples) (Arora et al., 2020). Many works (Allen-Zhu et al., 2019a;b; Arora et al., 2019a; Du et al., 2019b;a; Li & Liang, 2018; Zou et al., 2018; Cao & Gu, 2019) have since applied this lens to understand the optimization and generalization behavior of deep networks. However, these analyses of optimization and generalization do not directly apply to the pre-training and fine-tuning framework because (1) the network trained during FT is inherited and non-random; and (2) LMs are often trained with Adam, and the NTK formula only describes training an infinitely wide network with SGD. In this work, we handle the issue of a non-random (i.e., pre-trained) initialization by assuming that the pre-training task is sufficiently related to the downstream task (Definition 7.1), and we derive new kernels to model early-stage training with Adam (Section 4).

Theory of self-supervised learning and transfer learning. Existing theoretical works on transfer learning focus on linear probing and use the representation to provide guarantees on various tasks related to the original training data (Du et al., 2021; Tripuraneni et al., 2020; Wu et al., 2020). Additionally, Saunshi et al. (2021) studied autoregressive language models to rigorously characterized why prompting can improve zero-shot task performance, but their analysis precludes an investigation of FT. We focus on the masked language model pretraining objective, but it is worth noting that there are many works (Saunshi et al., 2019; Tosh et al., 2021a;b; Lee et al., 2021; Tsai et al., 2021)

studying transfer when pre-training with a contrastive objective. However, experiments on language modeling (Abnar et al., 2021) and contrastive learning (Saunshi et al., 2022) recently demonstrated that properties of transfer between self-supervised pre-training and supervised FT cannot be fully captured by model-agnostic analyses that directly relate the pre-training and downstream task errors. Kernel theory provides a principled optimization- and architecture-aware framework to analyze FT.

Optimization of transformers. Several works (Zhang et al., 2020; Liu et al., 2020a; Li et al., 2022) have documented issues with optimizing Transformer-based architectures with SGD instead of Adam. To study the unique properties of optimizing transformers with Adam, we derive a new kernel formula (Theorem 4.3) to capture early-stage training with Adam. We show results with this kernel and FT with Adam and SGD in Table 1.

Variants of fine-tuning methods. A standard way of fine-tuning pre-trained LMs as introduced in Radford et al. (2018); Devlin et al. (2019) is to add a linear classifier on top of a PT encoder and update all the parameters together. Subsequent work (Schick & Schütze, 2021; Gao et al., 2021) formulated downstream tasks as a language modeling problem (i.e., prompt-based FT) and demonstrated empirical success in low-data scenarios (see Liu et al. (2022) for a comprehensive survey). Another line of research studies parameter-efficient fine-tuning methods in which only a subset of model parameters are updated (Lester et al., 2021; Ben Zaken et al., 2022; Li & Liang, 2021) or the parameters updates are restricted to a low-dimensional subspace (Hu et al., 2021; Aghajanyan et al., 2021). We show that good eNTK performance arises only when studying prompt-based FT in Section 5 (Figure 1) and we later show in Section 6 that subspace-based fine-tuning methods such as LoRA (Hu et al., 2021) have a simple interpretation through the kernel.

3 PRELIMINARIES

3.1 KERNEL BEHAVIOR

It has been mathematically proven that training infinitely wide deep networks (with large Gaussian initialization) on small datasets can cause deep learning to turn into kernel-based learning. We are interested in identifying kernel behavior arising when training from an arbitrary initialization. Below, we adapt the definition of *lazy regime* (Woodworth et al., 2020) to an arbitrary initialization.

Definition 3.1 (Kernel Behavior). Consider a neural network $f(\xi; \theta)$ that takes input ξ and computes a scalar output² using θ as the parameters. Let θ_t be the parameters after t steps of training by a gradient-based optimization algorithm. We say this training process of the network demonstrates *kernel behavior* if the following properties are satisfied.

1. *Linearization*: The change of the network can be approximated by its first order Taylor expansion, i.e.,

$$f(\xi; \theta_t) - f(\xi; \theta_{t-1}) \approx \langle \nabla f(\xi; \theta_{t-1}), \theta_t - \theta_{t-1} \rangle;$$

2. *Fixed Features*: The gradient at step t is approximately the same as before training, i.e.,

$$\nabla f(\xi; \theta_t) \approx \nabla f(\xi; \theta_0).$$

∇f denotes the gradient of f w.r.t. θ . “Closeness to kernel behavior” is quantified using the difference in the quantities on the two sides of the \approx symbol. We formalize the approximations in Definition D.3.

Definition 3.2 (Kernel Analog). Suppose optimization of the parameters θ of a model f using the gradient-based update algorithm \mathcal{A} to minimize a loss $\ell : \mathbb{R}^2 \rightarrow \mathbb{R}$ exhibits kernel behavior (Definition 3.1). Then, we say that a kernel $\mathcal{K}^{(\mathcal{A})}$ is the *kernel analog* of the optimization algorithm \mathcal{A} if

$$f(\xi; \theta_t) - f(\xi; \theta_{t-1}) \approx -\eta \chi(f(\xi_t, \theta_t), y_t) \mathcal{K}^{(\mathcal{A})}(\xi, \xi_t), \forall t \geq 0 \quad (2)$$

where ξ_t, y_t is the training input and target label of step t , θ_t is the parameter at step t , $\chi(f, y) = \frac{\partial \ell(f, y)}{\partial f}$ is the derivative of the loss with respect to the model output.

²Note that for C -way classification, f is a vector in \mathbb{R}^C . We say f exhibits kernel behavior if the Linearization and Fixed Features properties hold for every component of f . The subsequent definition of a kernel analog also generalizes to a vector output component-wise.

We illustrate how the dynamics of an optimization algorithm that demonstrates kernel behavior relates to the kernel analog. Let \mathcal{A} be SGD. If SGD exhibits kernel behavior, then we can write how the function changes for a chosen input ξ as

$$f(\xi; \theta_{t+1}) - f(\xi; \theta_t) \approx \langle \nabla f(\xi; \theta_t), \theta_{t+1} - \theta_t \rangle = \langle \nabla f(\xi; \theta_t), -\eta \chi_t \nabla f(\xi_t; \theta_t) \rangle \approx -\eta \chi_t \mathcal{K}^{(\text{SGD})}(\xi, \xi_t),$$

where the approximations follow from the Linearization and Fixed Features property, respectively, and χ_t denotes $\chi_t(f(\xi_t, \theta_t), y_t)$. This construction immediately yields the standard NTK formula for $\mathcal{K}^{(\text{SGD})}$ derived in [Jacot et al. \(2018\)](#), which represents an input ξ as the resulting gradient $\nabla f(\xi; \theta_0)$.

Definition 3.3 (Neural Tangent Kernel $\mathcal{K}^{(\text{SGD})}$). $\mathcal{K}^{(\text{SGD})}(\xi, \xi') = \langle \nabla f(\xi; \theta_0), \nabla f(\xi'; \theta_0) \rangle$

Given an kernel \mathcal{K} , one can solve the classification problem by learning kernel coefficients α_i to minimize the empirical risk of $\sum_i \alpha_i \mathcal{K}(\cdot, \xi_i)$, where $\{\xi_i\}$ is the training data (see [Appendix A](#)). In [Section 4](#), we derive the kernel analog for SignGD (i.e., an early-stage approximation of Adam), and in [Section 5](#), we compare its eNTK performance against Adam FT. The eNTK computation relies on two design choices for the setting: (1) what the model output $f(\xi; \theta)$ is, and (2) which optimization algorithm \mathcal{A} is being studied. For a given setting, the eNTK can be computed directly using the kernel analog ([Definition 3.2](#)) of \mathcal{A} . We run experiments choosing \mathcal{A} as SGD or Adam and choosing f based on the fine-tuning setting.

3.2 PRE-TRAINING AND FINE-TUNING PARADIGM

We focus our attention on masked language models (MLMs), such as BERT ([Devlin et al., 2019](#)) and RoBERTa ([Liu et al., 2020b](#)), which are trained to minimize the cross-entropy loss on independently predicting masked tokens (i.e., a $|\mathcal{V}|$ -way classification task, where \mathcal{V} is the vocabulary). Given a text input s of length T from the pre-training distribution \mathcal{S}_{PT} , replace a small percentage (e.g., 15%) of tokens with [MASK] tokens. This masked input is then fed into the representation function $h : \mathcal{S}_{\text{PT}} \rightarrow T \times \mathbb{R}^n$ (e.g., a Transformer encoder) to produce a low-dimensional contextual embedding for each position in the input. The contextual embeddings are independently multiplied by a classifier head (i.e., word embeddings) $\Phi \in \mathbb{R}^{n \times |\mathcal{V}|}$ to produce logits that will be used to compute the probability of a token filling each masked position.

Using a PT model to solve downstream tasks effectively has been a highly active area of research. We focus on fine-tuning (FT) methods, which adapt the pre-trained model to a new input distribution \mathcal{S}_{FT} using additional training on the C -way downstream classification task.

1. **Standard FT** ([Devlin et al., 2019](#); [Liu et al., 2020b](#)): To solve a C -way downstream classification task, initialize and learn³ a new classifier head $\Gamma : \mathbb{R}^n \rightarrow \mathbb{R}^C$ on top of the contextual embedding of the [CLS], denoted $h_{[\text{CLS}]}$. In this case, the choice of $f : \mathcal{S}_{\text{FT}} \rightarrow \mathbb{R}^C$ for the eNTK construction is $f(s) = \Gamma(h_{[\text{CLS}]}(s))$.
2. **Prompt-based FT** ([Schick & Schütze, 2021](#); [Gao et al., 2021](#)): Add a natural language prompt (e.g. “This is [MASK].”) in addition to the task input to the downstream task, and use the pre-trained MLM to fill in the masked token. Compute the logits over task-relevant words (e.g., “great” and “terrible”) using the corresponding columns of Φ , denoted $\tilde{\Phi} \in \mathbb{R}^{n \times C}$. These logits will serve as surrogates to solve the downstream task. In this case, the choice of $f : \mathcal{S}_{\text{FT}} \rightarrow \mathbb{R}^C$ for the eNTK construction is $f(s) = \tilde{\Phi}^\top h_{[\text{MASK}]}(s)$.

4 KERNEL DERIVATION FOR ADAM

Computing the eNTK requires using the kernel analog ([Definition 3.2](#)) of the chosen optimization algorithm \mathcal{A} . We show that the kernel capturing training with Adam is an asymmetric SignGD kernel. Because FT requires relatively few steps, we model Adam updates with SignGD ([Ma et al., 2022](#); [Malladi et al., 2022](#)). Note that it is difficult to construct a long-term kernel analog for Adam, because the adaptivity causes the each update to depend on the entire gradient history.

³In our experiments, Standard FT corresponds to initializing Γ at the linear probing solution (i.e., training Γ on the downstream task while freezing all other layers) and then performing FT. We do this because when FT exhibits kernel behavior ([Definition 3.1](#)), it finds solutions close to initialization, and we hypothesize that the Γ learned during FT is closer to the linear probing solution than a random initialization.

Definition 4.1 (SignGD). SignGD is a gradient-based optimization algorithm that updates the parameters as $\theta_{t+1} = \theta_t - \eta \text{sign}(\nabla f(\xi_t; \theta_t))$, where sign is applied element-wise.

Definition 4.2 (Asymmetric SignGD Kernel). $\mathcal{K}^{(\text{A-SignGD})}(\xi, \xi') = \langle \nabla f(\xi; \theta_0), \text{sign}(\nabla f(\xi'; \theta_0)) \rangle$.

Theorem 4.3 (Informal version of Theorem D.4). *If a network is trained with SignGD (Definition 4.1) and the training exhibits kernel behavior (Definition 3.1), then the training dynamics can be characterized as*

$$f(\xi; \theta_t) - f(\xi; \theta_{t-1}) \approx -\eta \chi_t \mathcal{K}^{(\text{A-SignGD})}(\xi, \xi_t),$$

where χ_t is the derivative of the loss with respect to f at step t .

Proof sketch. By the Linearization property in Definition 3.1,

$$f(\xi; \theta_t) - f(\xi; \theta_{t-1}) \approx \langle \nabla f(\xi; \theta_t), \theta_t - \theta_{t-1} \rangle = -\eta \chi_t \langle \nabla f(\xi; \theta_t), \text{sign}(\nabla f(\xi_t; \theta_{t-1})) \rangle.$$

Then by the Fixed Features in Definition 3.1,

$$\langle \nabla f(\xi; \theta_t), \text{sign}(\nabla f(\xi_t; \theta_{t-1})) \rangle \approx \langle \nabla f(\xi; \theta_0), \text{sign}(\nabla f(\xi_t; \theta_0)) \rangle = \mathcal{K}^{(\text{A-SignGD})}(\xi, \xi_t). \quad \square$$

We solve the asymmetric kernel regression as suggested in He et al. (2022) (Appendix A.3), but the difficulties of solving the kernel regression problem with an asymmetric kernel motivate us to also use the symmetric SignGD kernel.

Definition 4.4 (SignGD Kernel). $\mathcal{K}^{(\text{SignGD})}(\xi, \xi') = \langle \text{sign}(\nabla f(\xi; \theta_0)), \text{sign}(\nabla f(\xi'; \theta_0)) \rangle$

5 EXPERIMENTS

We compute the eNTK as described in Section 3 for different optimization algorithms and FT settings. eNTK performance being comparable to FT performance is a necessary but not sufficient condition for FT to exhibit kernel behavior (Definition 3.1), so we also directly measure if the Linearization and Fixed Features properties hold (Section 5.3).

5.1 SETUP

Our experiments follow the few-shot setting from Gao et al. (2021) and use their manual prompt templates. We consider 12 NLP tasks, divided equally into 6 single sentence and 6 sentence pair datasets, which cover: sentiment analysis (SST-2, MR, CR); classifying an opinion’s polarity (MQPA) or subjectivity (Subj) or question type (TREC); natural language inference (MNLI, SNLI, QNLI, RTE); and paraphrase detection tasks (MRPC, QQP). For each task, we randomly sample 5 k -shot datasets with k training examples for each label. We use a pre-trained RoBERTa-base (Liu et al., 2020b) for all FT and eNTK experiments. Appendix A contains further implementation details.

5.2 KERNEL PERFORMANCE ON DOWNSTREAM TASKS

eNTK performance in standard and prompt-based FT. We measure the eNTK performance in the standard and prompt-based FT settings across SST-2, MR, CR, QNLI, QQP and RTE. (Figure 1). In the standard FT setting, $\mathcal{K}^{(\text{SGD})}$ and SGD FT demonstrate a gap of up to 15% absolute on tasks that exhibit only a 1% gap in the prompt-based setting. We explore the importance of the choice of prompt format in Appendix C.

Prompt-based SGD FT and Adam FT. We focus on the prompt-based FT setting (Table 1). We note that when doing prompt-based FT, Adam and SGD perform within 4% absolute of each other, furthering the discussion around the optimization of transformers with Adam versus SGD (Li et al., 2022; Zhang et al., 2020; Liu et al., 2020a).

Prompt-based eNTK across tasks. To study if the eNTK can solve a given task in the prompt-based FT setting, we compare SGD-FT to $\mathcal{K}^{(\text{SGD})}$ and Adam-FT to $\mathcal{K}^{(\text{A-SignGD})}$ and $\mathcal{K}^{(\text{SignGD})}$ in Table 1. We observe that for 8 out of 12 tasks, $\mathcal{K}^{(\text{SGD})}$ can achieve accuracy within 5% absolute of SGD FT for $k = 16$ and $k = 64$. Similarly, $\mathcal{K}^{(\text{SignGD})}$ or $\mathcal{K}^{(\text{A-SignGD})}$ can achieve accuracy comparable to Adam FT for 7 out of the 12 tasks. The difference between $\mathcal{K}^{(\text{SignGD})}$ and $\mathcal{K}^{(\text{A-SignGD})}$ is negligible on most tasks. We suggest the asymmetry of the latter may cause $\mathcal{K}^{(\text{A-SignGD})}$ to sometimes perform worse than $\mathcal{K}^{(\text{SignGD})}$ despite being the theoretically sound kernel analog (Theorem 4.3).

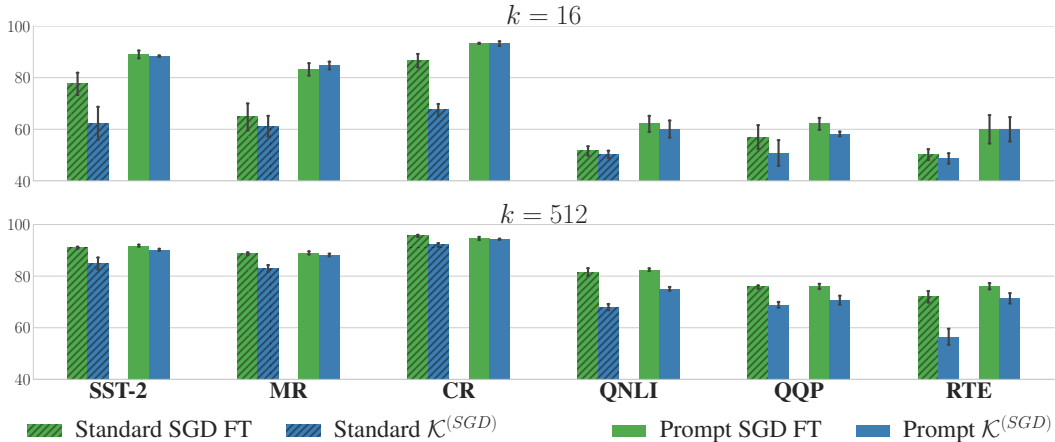


Figure 1: Comparing SGD-FT and $\mathcal{K}^{(SGD)}$ performance in the standard and the prompt-based FT settings (Section 3) suggests that kernel behavior (Definition 3.1 can only arise when using a prompt. In standard FT, we initialize the new classification head (i.e., Γ) using the linear probing solution. Performance is measured by accuracy, except for F1 in QQP, and is average over 5 random seeds.

When does the eNTK not match FT performance? The eNTK performs much worse than FT on all of the multi-class (i.e., TREC, MNLI, and SNLI) tasks, which we believe warrants further investigation. We conjecture that the eNTK cannot solve MNLI and SNLI despite solving binary entailment tasks (i.e., QNLI and RTE) because the prompt is less natural when considering the label word “Maybe” (see Appendix A.1 for prompt templates). One explanation of why the kernel analog sometimes outperforms FT is that certain batches may induce anomalous gradients that disrupt the FT trajectory, and the kernel can mitigate the effect of these examples by assigning small kernel coefficients to them.

5.3 MEASURING KERNEL BEHAVIOR

The eNTK matches the performance of prompted FT for many tasks (Table 1), suggesting that these tasks may induce kernel behavior (Definition 3.1). However, the kernel’s success may just be a coincidence. We take additional measurements to provide further empirical evidence that FT could be modeled as kernel behavior.

Linearization of the entire FT. If FT exhibits kernel behavior (Definition 3.1), then the function output after FT should be close to the first order Taylor expansion around the pre-trained model:

$$f(\xi; \theta_{FT}) \approx f(\xi; \theta_{PT}) + \langle \nabla f(\xi; \theta_{PT}), \theta_{FT} - \theta_{PT} \rangle$$

where θ_{PT} is the model parameters after pre-training, θ_{FT} is the model parameters after fine-tuning on the downstream task, and ξ is sampled from the test set. Figure 2 summarizes the results.

Pre-trained models perform significantly better than random on many single-sentence downstream tasks (e.g., SST-2, MR, and CR) but close to random on most sentence-pair tasks (e.g., QNLI, RTE, MRPC, and QQP). Subj, MNLI, and SNLI are outliers to this trend. Although pre-trained models perform much better than random on MNLI and SNLI, we find that the eNTK cannot solve these tasks very well (Table 1). Similarly, although the pre-trained model demonstrates near-random performance on QNLI and RTE, we find that the eNTK can solve these tasks. These findings suggest a deeper mystery around entailment tasks in particular.

The linearized model recovers a substantial amount of FT performance for SST-2, MR, CR, Subj, RTE, and QQP, all of which the eNTK could solve (Table 1). Although QNLI could be solved by the eNTK, the results suggest it does not induce the Linearization property of kernel behavior very strongly.

Fixed features. We also empirically test if the Fixed Features property (Definition 3.1) holds for tasks that the eNTK can solve. We measure the relative distance between $\mathcal{K}^{(SGD)}$ computed before

k -shot	Method	SST-2	MR	CR	MPQA	Subj	TREC
16	SGD-FT	89.0 _(1.5)	83.2 _(2.4)	93.3 _(0.2)	83.3 _(1.3)	88.5 _(2.6)	80.3 _(7.2)
	$\mathcal{K}^{(\text{SGD})}$	88.3 _(0.3)	84.7 _(1.5)	93.2 _(0.9)	76.4 _(2.7)	88.6 _(1.3)	56.0 _(9.2)
	Adam-FT	88.3 _(1.2)	81.3 _(6.1)	93.0 _(1.6)	82.8 _(2.2)	87.4 _(2.1)	79.6 _(6.1)
64	$\mathcal{K}^{(\text{SignGD})}$	88.3 _(0.5)	84.3 _(1.5)	93.7 _(0.5)	76.7 _(3.3)	89.2 _(2.0)	58.1 _(6.5)
	$\mathcal{K}^{(\text{A-SignGD})}$	88.3 _(0.4)	84.9 _(1.1)	93.4 _(0.5)	74.6 _(3.5)	88.6 _(1.8)	22.7 _(2.8)
	SGD-FT	89.7 _(0.4)	85.6 _(1.1)	94.3 _(0.5)	84.8 _(0.8)	92.9 _(0.5)	93.2 _(1.0)
64	$\mathcal{K}^{(\text{SGD})}$	89.2 _(1.0)	86.4 _(0.6)	93.7 _(0.4)	81.2 _(0.9)	91.4 _(0.7)	77.8 _(2.3)
	Adam-FT	89.3 _(0.7)	86.0 _(0.4)	93.7 _(0.8)	84.6 _(0.9)	92.7 _(0.6)	92.6 _(1.3)
	$\mathcal{K}^{(\text{SignGD})}$	89.1 _(0.5)	85.6 _(1.0)	93.9 _(0.2)	79.0 _(5.8)	92.4 _(0.5)	82.0 _(1.4)
64	$\mathcal{K}^{(\text{A-SignGD})}$	88.9 _(0.9)	85.6 _(1.0)	94.0 _(0.3)	81.8 _(1.1)	91.8 _(1.1)	21.0 _(4.3)

(a) Single-sentence tasks

k -shot	Method	MNLI	SNLI	QNLI	RTE	MRPC	QQP
16	SGD-FT	59.2 _(2.7)	65.7 _(2.7)	62.1 _(3.1)	60.0 _(5.5)	73.9 _(2.7)	62.1 _(2.3)
	$\mathcal{K}^{(\text{SGD})}$	53.0 _(3.0)	57.8 _(2.3)	60.1 _(3.3)	60.0 _(4.7)	73.4 _(5.6)	58.2 _(0.9)
	Adam-FT	56.8 _(2.9)	64.6 _(4.1)	63.1 _(3.5)	57.6 _(6.3)	77.6 _(3.1)	61.8 _(4.5)
64	$\mathcal{K}^{(\text{SignGD})}$	53.8 _(1.2)	54.9 _(2.7)	59.5 _(3.1)	55.4 _(4.2)	75.6 _(1.2)	60.7 _(2.2)
	$\mathcal{K}^{(\text{A-SignGD})}$	51.9 _(4.0)	54.9 _(3.1)	56.0 _(1.9)	59.8 _(4.0)	75.2 _(2.6)	59.4 _(2.0)
	SGD-FT	68.7 _(1.7)	77.3 _(0.9)	72.8 _(2.2)	68.9 _(2.5)	82.8 _(1.2)	69.2 _(1.3)
64	$\mathcal{K}^{(\text{SGD})}$	60.4 _(1.8)	65.5 _(1.6)	67.3 _(1.6)	66.5 _(2.5)	79.2 _(2.5)	66.4 _(1.7)
	Adam-FT	67.9 _(1.0)	76.9 _(1.4)	74.2 _(3.2)	67.3 _(2.7)	80.9 _(1.2)	69.8 _(0.6)
	$\mathcal{K}^{(\text{SignGD})}$	60.8 _(1.7)	64.1 _(2.3)	65.4 _(1.7)	63.8 _(1.8)	77.4 _(2.3)	63.7 _(4.4)
64	$\mathcal{K}^{(\text{A-SignGD})}$	58.5 _(1.7)	66.8 _(1.1)	66.5 _(1.1)	63.8 _(2.2)	77.3 _(2.0)	66.1 _(3.4)

(b) Sentence-pair tasks

Table 1: Performance achieved by prompt-based FT and prompt-based eNTKs with different formulas on the LM-BFF test set (Gao et al., 2021). The eNTK performs comparably to the analogous FT on many tasks but fails on multi-class tasks (i.e., TREC, SNLI, and MNLI). Performance is measure by average test accuracy over 5 k -shot splits for all tasks except MRPC and QQP, where it is F1.

and after FT and record the average element-wise distance in Table 7. A smaller distance indicates that the Fixed Features property is more likely to hold. We see that tasks that the eNTK can solve exhibit relatively low (i.e., less than 1) distances.

6 EFFICACY OF SUBSPACE-BASED FINE-TUNING METHODS

A surprising feature of fine-tuning is the efficacy of subspace-based fine-tuning methods, which apply updates to only a low-dimensional subspace of the high-dimensional model parameter space during fine-tuning. Although theoretical characterization of these methods seems complex, the kernel view admits a simple interpretation. We straightforwardly apply the classical Johnson-Lindenstrauss, or JL, lemma in Johnson (1984), which guarantees inner product preservation under random projections, to suggest why two subspace-based fine-tuning methods, LoRA (Hu et al., 2021) and IntrinsicDimension FT (Li et al., 2018; Aghajanyan et al., 2021)), work.

Definition 6.1 (\mathcal{A} -LoRA FT (Hu et al., 2021)). Let \mathcal{A} be a gradient-based optimization algorithm. For every weight matrix $W \in \mathbb{R}^{m \times n}$, choose $k \ll m$ and initialize $A \in \mathbb{R}^{m \times k}$ with i.i.d. mean-0 Gaussian values and $B \in \mathbb{R}^{k \times n}$ as 0. Set the weight to be $W + AB$. To fine-tune, fix W at its pre-trained value and train only A and B using \mathcal{A} .

Definition 6.2 (\mathcal{A} -IntrinsicDimension FT (Li et al., 2018; Aghajanyan et al., 2021)). Let $\theta \in \mathbb{R}^M$ be the model parameters and fix a random projection $\Pi \in \mathbb{R}^{M \times k}$. Set θ to $\theta + \Pi\hat{\theta}$, where $\hat{\theta} \in \mathbb{R}^k$. To fine-tune, fix θ at its pre-trained value and only train $\hat{\theta}$.

Analysis of these methods involves reasoning about the kernel, so we are interested in studying prompt-based FT, where we have empirical (Section 5) and theoretical (Section 7) evidence that FT

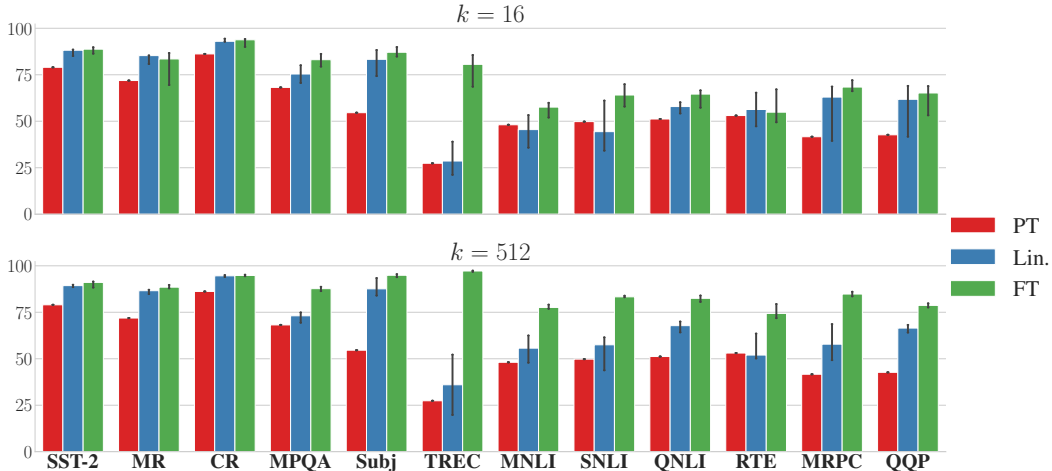


Figure 2: Accuracies of zero-shot pre-trained model (PT), linearized model (Lin., see Definition 3.1) and fine-tuned model (FT). Tasks that induce the Linearization property of kernel behavior (Definition 3.1) will show that Lin. performance recovers a substantial amount of the FT performance. For each k , we plot the median and range of the test accuracies across 5 seeds and data splits.

can be described by kernel behavior (Definition 3.1). In particular, we show that if SGD FT exhibits kernel behavior, then performing SGD-LoRA or SGD-IntrinsicDimension FT using a sufficiently large k preserves the kernel.

Theorem 6.3 (LoRA and IntrinsicDimension FT preserve $\mathcal{K}^{(SGD)}$, informal version of Theorem E.5). *Let $\mathcal{K}^{(SGD)}$ be the kernel analog (Definition 3.2) to SGD FT, $\mathcal{K}_{LoRA}^{(SGD)}$ be the kernel analog to SGD-LoRA FT (Definition 6.1), and $\mathcal{K}_{ID}^{(SGD)}$ be the kernel analog to SGD-IntrinsicDimension FT (Definition 6.2) on a downstream task Ξ . Then, with high probability, $(\mathcal{K}_{LoRA}^{(SGD)}(i, j) - \mathcal{K}_{ID}^{(SGD)}(i, j)) / \mathcal{K}^{(SGD)}(i, j) \approx 0$ and $\mathcal{K}_{ID}^{(SGD)}(i, j) \approx \mathcal{K}^{(SGD)}(i, j)$ for all $i, j \in [N]$.*

Proof sketch. Consider an individual layer in the network and inputs $\xi, \xi' \in \Xi$ to the downstream task. LoRA randomly projects $\nabla_B f(\xi; \theta)$ and $\nabla_B f(\xi'; \theta)$, where ∇_B denotes the gradient with respect to B , and does not modify the gradient to A , since B is initialized to zero. The rest of the proof for LoRA and the proof for IntrinsicDimension FT follows from applying JL to all such pairs ξ, ξ' to show the inner product, which determines the kernel entry, is preserved. \square

Remark 6.4. Theorem 6.3 states that the kernel analog of SGD FT is unchanged by LoRA in both prompt-based and standard FT. However, the theorem only provides an explanation for the success of \mathcal{A} -LoRA FT when \mathcal{A} FT exhibits kernel behavior. Therefore, as per Table 5, we consider this theorem to only be meaningful when considering prompt-based SGD and prompt-based SGD-LoRA.

Experimental results in Table 8 verify that prompted SGD FT and prompted LoRA-SGD FT achieve similar performance on several downstream tasks, and $\mathcal{K}_{LoRA}^{(SGD)}$ achieves performance similar to $\mathcal{K}^{(SGD)}$.

7 THEORY: PROMPT-BASED FINE-TUNING CAN EXHIBIT KERNEL BEHAVIOR

We give a plausible mechanism for how, as network width grows large, prompt-based FT can exhibit kernel behavior (Definition 3.1) despite starting from a non-random initialization. We place no limits on the size of the fine-tuning training dataset. The theory focuses on the prompt-based setting (Section 3), since we did not find empirical evidence of kernel behavior in the standard setting (Figure 1). Without loss of generality, we assume the network output is a scalar, and the pre-trained network is fine-tuned directly without any modification.

Definition 7.1 (Solvable Task in the Infinite-Width Limit). Let $\{f^n(\cdot; \theta_0^n)\}_{n>0}$ be a series of models where $f^n(\cdot; \theta_0^n)$ represents a pre-trained model of width n . We say a downstream task Ξ is *solvable in*

the infinite-width limit if, for any constant t and any $(\xi, y) \in \Xi$,

$$\lim_{n \rightarrow \infty} \chi(f^n(\xi; \theta_t^n), y) = 0, \quad (3)$$

where θ_t^n is the parameter of f^n after t steps of fine-tuning on the downstream task. We abuse notation and to denote $\{f^n(\cdot; \theta_t^n)\}_{n>0}$ as $f(\cdot; \theta_t)$, so eq. (3) becomes $\chi(f(\xi; \theta_t), y) = o(1)$.

Remark 7.2. The notion of solvable tasks is analogous to *natural tasks* (Saunshi et al., 2021), which are defined as tasks that can be solved by optimal autoregressive models using a complete-the-sentence perspective. Since $\chi(f(\xi; \theta_t), y)$ is assumed to go to 0 as width increases, there will be finite width values where it is small enough for fine-tuning to still be close to kernel behavior.

Although Definition 7.1 is asymptotic, we can design and run a cheap empirical test on a given architecture and downstream task Ξ : measuring $\chi(f(\xi, \theta_{PT}), y)$ for two networks of different widths without making any gradient updates. Table 2 shows that the necessary condition holds for most tasks the eNTK can solve, suggesting that our theoretical mechanism is plausible.⁴

Model size	SST-2	MR	CR	MPQA	Subj	QNLI	RTE	MRPC	QQP
Base ($n = 768$)	0.32	0.32	0.26	0.38	0.43	0.48	0.48	0.56	0.49
Large ($n = 1024$)	0.32	0.25	0.25	0.40	0.46	0.48	0.47	0.52	0.52

Table 2: We measure χ (Definition 3.2) in the prompt-based FT setting for RoBERTa-base and RoBERTa-large. A decrease in the χ value when going from RoBERTa-base to RoBERTa-large indicates the task may be solvable in the infinite-width limit (Definition 7.1). We find that for most tasks the eNTK can solve (Table 1), χ decreases as model width grows.

To study the behavior of fine-tuning one also needs to make assumptions about parameters that resulted from the pre-training. We assume that during pre-training, the network can be written as a Tensor Program (Yang, 2019; 2020a;b), which is sufficiently general to allow our theory to describe many complex architectures (e.g., Transformers).

Theorem 7.3 (Informal version of Theorem D.5). *Assume the downstream task Ξ is solvable in the infinite-width limit with a pre-trained model f , and f satisfies Assumption D.2. Then prompt-based FT of f will exhibit kernel behavior (Definition 3.1).*

Proof Sketch of Theorem 7.3. Let ξ_t be the training example at step t of fine-tuning. Define $\chi_t = \chi(\xi_t, f(\xi_t; \theta_{t-1}))$, and $\boldsymbol{\chi} = [\chi_1, \dots, \chi_t]^\top$. The first order term of the Taylor expansion⁵ of $f(\xi; \theta_t) - f(\xi; \theta_0)$ around $\boldsymbol{\chi} = 0$ is

$$\begin{aligned} \sum_{\tau=1}^t \chi_\tau \left(\frac{\partial(f(\xi; \theta_t) - f(\xi; \theta_0))}{\partial \chi_\tau} \right) \Big|_{\boldsymbol{\chi}=0} &= \sum_{\tau=1}^t \chi_\tau \left(\frac{\partial f(\xi; \theta_t)}{\partial \chi_\tau} \right) \Big|_{\boldsymbol{\chi}=0} \\ &= \sum_{\tau=1}^t \chi_\tau \left(\left\langle \nabla f(\xi; \theta_t), \frac{\partial \theta_t}{\partial \chi_\tau} \right\rangle \right) \Big|_{\boldsymbol{\chi}=0} \quad (\text{chain rule}) \\ &= \sum_{\tau=1}^t -\eta \chi_\tau \mathcal{K}(\xi, \xi_\tau) \quad (\nabla f(\xi; \theta_t)|_{\boldsymbol{\chi}=0} = \nabla f(\xi; \theta_0)) \end{aligned}$$

The higher order terms have at least two χ_τ in each term. By Tensor Programs, we show that the first order term of the Taylor expansion is $\Theta(\|\boldsymbol{\chi}\|_1)$, which dominates the higher order terms of $O(\|\boldsymbol{\chi}\|_1^2)$ when taking the model to its infinite width limit. Therefore, we have proved that $f(\xi; \theta_t) - f(\xi; \theta_0) \approx \sum_{\tau=1}^t -\eta \chi_\tau \mathcal{K}(\xi, \xi_\tau)$ following eq. (2) in Definition 3.2. By Tensor Programs, we can prove eq. (2) also implies Definition 3.1. \square

⁴QQP and Subj are the exceptions. SST-2 and QNLI show no change in χ : this may be because the increase in width from $n = 768$ to $n = 1024$ is not large enough for χ to measurably decay.

⁵Assume χ_1, \dots, χ_t are independent of each other.

8 CONCLUSION

We use NTKs to mathematically formalize the general intuition that fine-tuning pretrained language models to solve downstream tasks requires only a “small change.” Extensive experiments on 12 NLU tasks demonstrate that prompt-based FT is much more likely to exhibit kernel behavior (Definition 3.1) than standard FT (Figure 1). Further experiments in the prompt-based FT setting using a newly derived kernel for Adam (Definition 4.2, see Theorem 4.3) demonstrate that the eNTK can match the performance of FT on many tasks. On the tasks that eNTK can solve, measurements in Section 5.3 suggest that prompt-based FT does exhibit kernel behavior. We demonstrate one possible use of the kernel view to explain empirical phenomena by applying it to understand subspace-based fine-tuning methods (Section 6), and we note that the kernel has many mathematically useful properties that can aid design and study of parameter-efficient fine-tuning methods. Moreover, one can use the kernel analog to study the inductive bias of FT, as was done for gradient descent from a random initialization in the past (Allen-Zhu et al., 2019b;a; Li & Liang, 2018). We provide a first-cut theoretical analysis in Section 7 as to why prompt-based fine-tuning can exhibit kernel behavior.

ACKNOWLEDGEMENTS

We thank Tianyu Gao, Wei Hu, Kaifeng Lyu, Abhishek Panigrahi, Nikunj Saunshi, Mengzhou Xia, and Greg Yang for their helpful comments and discussion. This work is funded by NSF, ONR, Simons Foundation, DARPA and SRC.

REFERENCES

- Samira Abnar, Mostafa Dehghani, Behnam Neyshabur, and Hanie Sedghi. Exploring the limits of large scale pre-training, 2021. URL <https://arxiv.org/abs/2110.02095>.
- Armen Aghajanyan, Sonal Gupta, and Luke Zettlemoyer. Intrinsic dimensionality explains the effectiveness of language model fine-tuning. In *Proceedings of the 59th Annual Meeting of the Association for Computational Linguistics and the 11th International Joint Conference on Natural Language Processing (Volume 1: Long Papers)*, pp. 7319–7328, Online, August 2021. Association for Computational Linguistics. doi: 10.18653/v1/2021.acl-long.568. URL <https://aclanthology.org/2021.acl-long.568>.
- Zeyuan Allen-Zhu, Yuanzhi Li, and Yingyu Liang. Learning and generalization in overparameterized neural networks, going beyond two layers. In *Advances in Neural Information Processing Systems*, volume 32. Curran Associates, Inc., 2019a. URL <https://proceedings.neurips.cc/paper/2019/file/62dad6e273d32235ae02b7d321578ee8-Paper.pdf>.
- Zeyuan Allen-Zhu, Yuanzhi Li, and Zhao Song. A convergence theory for deep learning via overparameterization. In *Proceedings of the 36th International Conference on Machine Learning*, volume 97 of *Proceedings of Machine Learning Research*, pp. 242–252. PMLR, 09–15 Jun 2019b. URL <https://proceedings.mlr.press/v97/allen-zhu19a.html>.
- Sanjeev Arora, Simon Du, Wei Hu, Zhiyuan Li, and Ruosong Wang. Fine-grained analysis of optimization and generalization for overparameterized two-layer neural networks. In *Proceedings of the 36th International Conference on Machine Learning*, volume 97 of *Proceedings of Machine Learning Research*, pp. 322–332. PMLR, 09–15 Jun 2019a. URL <https://proceedings.mlr.press/v97/arora19a.html>.
- Sanjeev Arora, Simon S Du, Wei Hu, Zhiyuan Li, Russ R Salakhutdinov, and Ruosong Wang. On exact computation with an infinitely wide neural net. In *Advances in Neural Information Processing Systems*, volume 32. Curran Associates, Inc., 2019b. URL <https://proceedings.neurips.cc/paper/2019/file/dbc4d84bfcfe2284ba11befb853a8c4-Paper.pdf>.
- Sanjeev Arora, Simon S. Du, Zhiyuan Li, Ruslan Salakhutdinov, Ruosong Wang, and Dingli Yu. Harnessing the power of infinitely wide deep nets on small-data tasks. In *International Conference on Learning Representations*, 2020. URL <https://openreview.net/forum?id=rkl8sJBYvH>.

- Roy Bar Haim, Ido Dagan, Bill Dolan, Lisa Ferro, Danilo Giampiccolo, Bernardo Magnini, and Idan Szpektor. The second PASCAL recognising textual entailment challenge. 2006. URL <https://citeseerx.ist.psu.edu/viewdoc/download?doi=10.1.1.60.8552&rep=rep1&type=pdf>.
- Elad Ben Zaken, Yoav Goldberg, and Shauli Ravfogel. BitFit: Simple parameter-efficient fine-tuning for transformer-based masked language-models. In *Proceedings of the 60th Annual Meeting of the Association for Computational Linguistics (Volume 2: Short Papers)*, pp. 1–9, Dublin, Ireland, May 2022. Association for Computational Linguistics. doi: 10.18653/v1/2022.acl-short.1. URL <https://aclanthology.org/2022.acl-short.1>.
- Luisa Bentivogli, Peter Clark, Ido Dagan, and Danilo Giampiccolo. The fifth PASCAL recognizing textual entailment challenge. In *TAC*, 2009. URL <https://citeseerx.ist.psu.edu/viewdoc/download?doi=10.1.1.232.1231&rep=rep1&type=pdf>.
- Samuel R. Bowman, Gabor Angeli, Christopher Potts, and Christopher D. Manning. A large annotated corpus for learning natural language inference. In *Proceedings of the 2015 Conference on Empirical Methods in Natural Language Processing*, pp. 632–642, Lisbon, Portugal, September 2015. Association for Computational Linguistics. doi: 10.18653/v1/D15-1075. URL <https://aclanthology.org/D15-1075>.
- Yuan Cao and Quanquan Gu. Generalization bounds of stochastic gradient descent for wide and deep neural networks. In *Advances in Neural Information Processing Systems*, volume 32. Curran Associates, Inc., 2019. URL <https://proceedings.neurips.cc/paper/2019/file/cf9dc5e4e194fc21f397b4cac9cc3ae9-Paper.pdf>.
- Kevin Clark, Minh-Thang Luong, Quoc V. Le, and Christopher D. Manning. Electra: Pre-training text encoders as discriminators rather than generators. In *International Conference on Learning Representations*, 2020. URL <https://openreview.net/forum?id=r1xMH1BtvB>.
- Ido Dagan, Oren Glickman, and Bernardo Magnini. The PASCAL recognising textual entailment challenge. In *the First International Conference on Machine Learning Challenges: Evaluating Predictive Uncertainty Visual Object Classification, and Recognizing Textual Entailment*, 2005. URL <https://kdd.cs.ksu.edu/Courses/Fall-2008/CIS798/Handouts/06-dagan05pascal.pdf>.
- Jacob Devlin, Ming-Wei Chang, Kenton Lee, and Kristina Toutanova. Bert: Pre-training of deep bidirectional transformers for language understanding. In *North American Chapter of the Association for Computational Linguistics (NAACL)*, pp. 4171–4186, 2019.
- William B. Dolan and Chris Brockett. Automatically constructing a corpus of sentential paraphrases. In *the Third International Workshop on Paraphrasing (IWP2005)*, 2005. URL <https://aclanthology.org/I05-5002.pdf>.
- Simon Du, Jason Lee, Haochuan Li, Liwei Wang, and Xiyu Zhai. Gradient descent finds global minima of deep neural networks. In *Proceedings of the 36th International Conference on Machine Learning*, volume 97 of *Proceedings of Machine Learning Research*, pp. 1675–1685. PMLR, 09–15 Jun 2019a. URL <https://proceedings.mlr.press/v97/du19c.html>.
- Simon S. Du, Xiyu Zhai, Barnabas Poczos, and Aarti Singh. Gradient descent provably optimizes over-parameterized neural networks. In *International Conference on Learning Representations*, 2019b. URL <https://openreview.net/forum?id=S1eK3i09YQ>.
- Simon Shaolei Du, Wei Hu, Sham M. Kakade, Jason D. Lee, and Qi Lei. Few-shot learning via learning the representation, provably. In *International Conference on Learning Representations*, 2021. URL <https://openreview.net/forum?id=pW2Q2xLwIMD>.
- Tianyu Gao, Adam Fisch, and Danqi Chen. Making pre-trained language models better few-shot learners. In *Association for Computational Linguistics (ACL)*, pp. 3816–3830, 2021.
- Danilo Giampiccolo, Bernardo Magnini, Ido Dagan, and Bill Dolan. The third PASCAL recognizing textual entailment challenge. In *the ACL-PASCAL Workshop on Textual Entailment and Paraphrasing*, 2007. URL <https://aclanthology.org/W07-1401.pdf>.

- Horace He and Richard Zou. functorch: Jax-like composable function transforms for pytorch. <https://github.com/pytorch/functorch>, 2021.
- Mingzhen He, Fan He, Lei Shi, Xiaolin Huang, and Johan A. K. Suykens. Learning with asymmetric kernels: Least squares and feature interpretation, 2022. URL <https://arxiv.org/abs/2202.01397>.
- Edward J. Hu, Yelong Shen, Phillip Wallis, Zeyuan Allen-Zhu, Yuanzhi Li, Shean Wang, Lu Wang, and Weizhu Chen. Lora: Low-rank adaptation of large language models, 2021. URL <https://arxiv.org/abs/2106.09685>.
- Minqing Hu and Bing Liu. Mining and summarizing customer reviews. In *ACM SIGKDD international conference on Knowledge discovery and data mining*, 2004.
- Arthur Jacot, Franck Gabriel, and Clement Hongler. Neural tangent kernel: Convergence and generalization in neural networks. In *Advances in Neural Information Processing Systems*, volume 31. Curran Associates, Inc., 2018. URL <https://proceedings.neurips.cc/paper/2018/file/5a4be1fa34e62bb8a6ec6b91d2462f5a-Paper.pdf>.
- William B Johnson. Extensions of lipschitz mappings into a hilbert space. *Contemp. Math.*, 26: 189–206, 1984.
- Mandar Joshi, Danqi Chen, Yinhan Liu, Daniel S Weld, Luke Zettlemoyer, and Omer Levy. SpanBERT: Improving pre-training by representing and predicting spans. *Transactions of the Association of Computational Linguistics (ACL)*, 2020.
- Diederik P. Kingma and Jimmy Ba. Adam: A method for stochastic optimization. In *ICLR (Poster)*, 2015. URL <http://arxiv.org/abs/1412.6980>.
- Jason D Lee, Qi Lei, Nikunj Saunshi, and JIACHENG ZHUO. Predicting what you already know helps: Provable self-supervised learning. In *Advances in Neural Information Processing Systems*, volume 34, pp. 309–323. Curran Associates, Inc., 2021. URL <https://proceedings.neurips.cc/paper/2021/file/02e656adee09f8394b402d9958389b7d-Paper.pdf>.
- Brian Lester, Rami Al-Rfou, and Noah Constant. The power of scale for parameter-efficient prompt tuning. In *Empirical Methods in Natural Language Processing (EMNLP)*, pp. 3045–3059, 2021.
- Chunyuan Li, Heerad Farkhor, Rosanne Liu, and Jason Yosinski. Measuring the intrinsic dimension of objective landscapes. In *International Conference on Learning Representations*, 2018. URL <https://openreview.net/forum?id=ryup8-WCW>.
- Xiang Lisa Li and Percy Liang. Prefix-tuning: Optimizing continuous prompts for generation. In *Proceedings of the 59th Annual Meeting of the Association for Computational Linguistics and the 11th International Joint Conference on Natural Language Processing (Volume 1: Long Papers)*, pp. 4582–4597, Online, August 2021. Association for Computational Linguistics. doi: 10.18653/v1/2021.acl-long.353. URL <https://aclanthology.org/2021.acl-long.353>.
- Yuanzhi Li and Yingyu Liang. Learning overparameterized neural networks via stochastic gradient descent on structured data. In *Advances in Neural Information Processing Systems*, volume 31. Curran Associates, Inc., 2018. URL <https://proceedings.neurips.cc/paper/2018/file/54fe976ba170c19ebae453679b362263-Paper.pdf>.
- Zhiyuan Li, Srinadh Bhojanapalli, Manzil Zaheer, Sashank Reddi, and Sanjiv Kumar. Robust training of neural networks using scale invariant architectures. In *Proceedings of the 39th International Conference on Machine Learning*, volume 162 of *Proceedings of Machine Learning Research*, pp. 12656–12684. PMLR, 17–23 Jul 2022. URL <https://proceedings.mlr.press/v162/li22b.html>.
- Liyuan Liu, Xiaodong Liu, Jianfeng Gao, Weizhu Chen, and Jiawei Han. Understanding the difficulty of training transformers. In *Proceedings of the 2020 Conference on Empirical Methods in Natural Language Processing (EMNLP)*, pp. 5747–5763, Online, November 2020a. Association for Computational Linguistics. doi: 10.18653/v1/2020.emnlp-main.463. URL <https://aclanthology.org/2020.emnlp-main.463>.

- Pengfei Liu, Weizhe Yuan, Jinlan Fu, Zhengbao Jiang, Hiroaki Hayashi, and Graham Neubig. Pre-train, prompt, and predict: A systematic survey of prompting methods in natural language processing. *ACM Comput. Surv.*, aug 2022. ISSN 0360-0300. doi: 10.1145/3560815. URL <https://doi.org/10.1145/3560815>. Just Accepted.
- Yinhan Liu, Myle Ott, Naman Goyal, Jingfei Du, Mandar Joshi, Danqi Chen, Omer Levy, Mike Lewis, Luke Zettlemoyer, and Veselin Stoyanov. Ro{bert}a: A robustly optimized {bert} pretraining approach, 2020b. URL <https://openreview.net/forum?id=SyxS0T4tvS>.
- Robert Logan IV, Ivana Balazevic, Eric Wallace, Fabio Petroni, Sameer Singh, and Sebastian Riedel. Cutting down on prompts and parameters: Simple few-shot learning with language models. In *Findings of the Association for Computational Linguistics: ACL 2022*, pp. 2824–2835, Dublin, Ireland, May 2022. Association for Computational Linguistics. doi: 10.18653/v1/2022.findings-acl.222. URL <https://aclanthology.org/2022.findings-acl.222>.
- Chao Ma, Lei Wu, and Weinan E. A qualitative study of the dynamic behavior for adaptive gradient algorithms. In *Proceedings of the 2nd Mathematical and Scientific Machine Learning Conference*, volume 145 of *Proceedings of Machine Learning Research*, pp. 671–692. PMLR, 16–19 Aug 2022. URL <https://proceedings.mlr.press/v145/ma22a.html>.
- Sadhika Malladi, Kaifeng Lyu, Abhishek Panigrahi, and Sanjeev Arora. On the sdes and scaling rules for adaptive gradient algorithms, 2022. URL <https://arxiv.org/abs/2205.10287>.
- Roman Novak, Jascha Sohl-Dickstein, and Samuel S Schoenholz. Fast finite width neural tangent kernel. In *Proceedings of the 39th International Conference on Machine Learning*, volume 162 of *Proceedings of Machine Learning Research*, pp. 17018–17044. PMLR, 17–23 Jul 2022. URL <https://proceedings.mlr.press/v162/novak22a.html>.
- Bo Pang and Lillian Lee. A sentimental education: Sentiment analysis using subjectivity summarization based on minimum cuts. In *Association for Computational Linguistics (ACL)*, 2004.
- Bo Pang and Lillian Lee. Seeing stars: Exploiting class relationships for sentiment categorization with respect to rating scales. In *Association for Computational Linguistics (ACL)*, 2005.
- Alec Radford, Karthik Narasimhan, Tim Salimans, Ilya Sutskever, et al. Improving language understanding by generative pre-training. 2018.
- Colin Raffel, Noam Shazeer, Adam Roberts, Katherine Lee, Sharan Narang, Michael Matena, Yanqi Zhou, Wei Li, Peter J Liu, et al. Exploring the limits of transfer learning with a unified text-to-text transformer. *J. Mach. Learn. Res.*, 21(140):1–67, 2020.
- Pranav Rajpurkar, Jian Zhang, Konstantin Lopyrev, and Percy Liang. SQuAD: 100,000+ questions for machine comprehension of text. In *Empirical Methods in Natural Language Processing (EMNLP)*, 2016. URL <https://aclanthology.org/D16-1264/>.
- Nikunj Saunshi, Orestis Plevrakis, Sanjeev Arora, Mikhail Khodak, and Hrishikesh Khandeparkar. A theoretical analysis of contrastive unsupervised representation learning. In *Proceedings of the 36th International Conference on Machine Learning*, volume 97 of *Proceedings of Machine Learning Research*, pp. 5628–5637. PMLR, 09–15 Jun 2019. URL <https://proceedings.mlr.press/v97/saunshi19a.html>.
- Nikunj Saunshi, Sadhika Malladi, and Sanjeev Arora. A mathematical exploration of why language models help solve downstream tasks. In *International Conference on Learning Representations*, 2021. URL <https://openreview.net/forum?id=vVjIW3sEcls>.
- Nikunj Saunshi, Jordan Ash, Surbhi Goel, Dipendra Misra, Cyril Zhang, Sanjeev Arora, Sham Kakade, and Akshay Krishnamurthy. Understanding contrastive learning requires incorporating inductive biases. In *Proceedings of the 39th International Conference on Machine Learning*, volume 162 of *Proceedings of Machine Learning Research*, pp. 19250–19286. PMLR, 17–23 Jul 2022. URL <https://proceedings.mlr.press/v162/saunshi22a.html>.
- Timo Schick and Hinrich Schütze. Exploiting cloze-questions for few-shot text classification and natural language inference. In *European Chapter of the Association for Computational Linguistics (EACL)*, pp. 255–269, 2021.

- Richard Socher, Alex Perelygin, Jean Wu, Jason Chuang, Christopher D. Manning, Andrew Ng, and Christopher Potts. Recursive deep models for semantic compositionality over a sentiment treebank. In *Empirical Methods in Natural Language Processing (EMNLP)*, 2013. URL <https://aclanthology.org/D13-1170.pdf>.
- Christopher Tosh, Akshay Krishnamurthy, and Daniel Hsu. Contrastive learning, multi-view redundancy, and linear models. In *Proceedings of the 32nd International Conference on Algorithmic Learning Theory*, volume 132 of *Proceedings of Machine Learning Research*, pp. 1179–1206. PMLR, 16–19 Mar 2021a. URL <https://proceedings.mlr.press/v132/tosh21a.html>.
- Christopher Tosh, Akshay Krishnamurthy, and Daniel Hsu. Contrastive estimation reveals topic posterior information to linear models. *Journal of Machine Learning Research*, 22(281):1–31, 2021b. URL <http://jmlr.org/papers/v22/21-0089.html>.
- Nilesh Tripuraneni, Michael Jordan, and Chi Jin. On the theory of transfer learning: The importance of task diversity. In *Advances in Neural Information Processing Systems*, volume 33, pp. 7852–7862. Curran Associates, Inc., 2020. URL <https://proceedings.neurips.cc/paper/2020/file/59587bffe1c7846f3e34230141556ae-Paper.pdf>.
- Yao-Hung Hubert Tsai, Yue Wu, Ruslan Salakhutdinov, and Louis-Philippe Morency. Self-supervised learning from a multi-view perspective. In *International Conference on Learning Representations*, 2021. URL https://openreview.net/forum?id=-bdp_8Itjwp.
- Ashish Vaswani, Noam Shazeer, Niki Parmar, Jakob Uszkoreit, Llion Jones, Aidan N Gomez, Łukasz Kaiser, and Illia Polosukhin. Attention is all you need. *Advances in neural information processing systems*, 30, 2017.
- Ellen M Voorhees and Dawn M Tice. Building a question answering test collection. In *the 23rd annual international ACM SIGIR conference on Research and development in information retrieval*, 2000.
- Alex Wang, Amanpreet Singh, Julian Michael, Felix Hill, Omer Levy, and Samuel R Bowman. GLUE: A multi-task benchmark and analysis platform for natural language understanding. In *International Conference on Learning Representations (ICLR)*, 2019. URL <https://openreview.net/forum?id=rJ4km2R5t7>.
- Alexander Wei, Wei Hu, and Jacob Steinhardt. More than a toy: Random matrix models predict how real-world neural representations generalize. In *Proceedings of the 39th International Conference on Machine Learning*, volume 162, pp. 23549–23588. PMLR, 17–23 Jul 2022. URL <https://proceedings.mlr.press/v162/wei22a.html>.
- Janyce Wiebe, Theresa Wilson, and Claire Cardie. Annotating expressions of opinions and emotions in language. *Language resources and evaluation*, 39(2-3), 2005.
- Adina Williams, Nikita Nangia, and Samuel Bowman. A broad-coverage challenge corpus for sentence understanding through inference. In *North American Chapter of the Association for Computational Linguistics: Human Language Technologies (NAACL-HLT)*, 2018. URL <https://aclanthology.org/N18-1101.pdf>.
- Blake Woodworth, Suriya Gunasekar, Jason D. Lee, Edward Moroshko, Pedro Savarese, Itay Golan, Daniel Soudry, and Nathan Srebro. Kernel and rich regimes in overparametrized models. In *Proceedings of Thirty Third Conference on Learning Theory*, volume 125 of *Proceedings of Machine Learning Research*, pp. 3635–3673. PMLR, 09–12 Jul 2020. URL <https://proceedings.mlr.press/v125/woodworth20a.html>.
- Sen Wu, Hongyang R. Zhang, and Christopher Ré. Understanding and improving information transfer in multi-task learning. In *International Conference on Learning Representations*, 2020. URL <https://openreview.net/forum?id=SylzhkDtDB>.
- Greg Yang. Wide feedforward or recurrent neural networks of any architecture are gaussian processes. *Advances in Neural Information Processing Systems*, 32, 2019.

Greg Yang. Tensor programs ii: Neural tangent kernel for any architecture. *arXiv preprint arXiv:2006.14548*, 2020a.

Greg Yang. Tensor programs iii: Neural matrix laws. *arXiv preprint arXiv:2009.10685*, 2020b.

Greg Yang and Edward J Hu. Tensor programs iv: Feature learning in infinite-width neural networks. In *International Conference on Machine Learning*, pp. 11727–11737. PMLR, 2021.

Greg Yang and Etai Littwin. Tensor programs iib: Architectural universality of neural tangent kernel training dynamics. In *International Conference on Machine Learning*, pp. 11762–11772. PMLR, 2021.

Greg Yang, Edward J Hu, Igor Babuschkin, Szymon Sidor, Xiaodong Liu, David Farhi, Nick Ryder, Jakub Pachocki, Weizhu Chen, and Jianfeng Gao. Tensor programs v: Tuning large neural networks via zero-shot hyperparameter transfer. *arXiv preprint arXiv:2203.03466*, 2022.

Jingzhao Zhang, Sai Praneeth Karimireddy, Andreas Veit, Seungyeon Kim, Sashank Reddi, Sanjiv Kumar, and Suvrit Sra. Why are adaptive methods good for attention models? In *Advances in Neural Information Processing Systems*, volume 33, pp. 15383–15393. Curran Associates, Inc., 2020. URL <https://proceedings.neurips.cc/paper/2020/file/b05b57f6add810d3b7490866d74c0053-Paper.pdf>.

Difan Zou, Yuan Cao, Dongruo Zhou, and Quanquan Gu. Stochastic gradient descent optimizes over-parameterized deep relu networks, 2018. URL <https://arxiv.org/abs/1811.08888>.

A EXPERIMENTAL DETAILS

A.1 DATASETS AND PROMPTS

Dataset	C	#Train	#Test	Type	Prompt	
SST-2	2	6,920	872	sentiment	$\langle S_1 \rangle$ It was [MASK] .	{great, terrible}
MR	2	8,662	1,000	sentiment	$\langle S_1 \rangle$ It was [MASK] .	{great, terrible}
CR	2	3,175	500	sentiment	$\langle S_1 \rangle$ It was [MASK] .	{great, terrible}
MPQA	2	8,606	1,000	opinion polarity	$\langle S_1 \rangle$ It was [MASK] .	{great, terrible}
Subj	2	8,000	1,000	subjectivity	$\langle S_1 \rangle$ This is [MASK] .	{subjective, objective}
TREC	6	5,452	500	question cls.	[MASK] : $\langle S_1 \rangle$	{Description, Expression, Entity, Human, Location, Number}
MNLI	3	392,702	1,000	NLI	$\langle S_1 \rangle$? [MASK] , $\langle S_2 \rangle$	{Yes, Maybe, No}
SNLI	3	549,367	1,000	NLI	$\langle S_1 \rangle$? [MASK] , $\langle S_2 \rangle$	{Yes, Maybe, No}
QNLI	2	104,743	1,000	NLI	$\langle S_1 \rangle$? [MASK] , $\langle S_2 \rangle$	{Yes, No}
RTE	2	2,490	277	NLI	$\langle S_1 \rangle$? [MASK] , $\langle S_2 \rangle$	{Yes, No}
MRPC	2	3,668	408	paraphrase	$\langle S_1 \rangle$ [MASK] , $\langle S_2 \rangle$	{Yes, No}
QQP	2	363,846	1,000	paraphrase	$\langle S_1 \rangle$ [MASK] , $\langle S_2 \rangle$	{Yes, No}

Table 3: The statistics and prompts of the datasets we used in our experiments. The choices of prompts are from Gao et al. (2021) which include a template, and a set of label words that are used to fill in the [MASK] token. $\langle S_1 \rangle$ and $\langle S_2 \rangle$ refer to the first and the second (if any) input sentence.

Table 3 shows the set of downstream tasks, which are adapted from Gao et al. (2021). We consider 6 single sentence classification datasets (SST-2 (Socher et al., 2013), MR (Pang & Lee, 2005), CR (Hu & Liu, 2004), MPQA (Wiebe et al., 2005), Subj (Pang & Lee, 2004) and TREC (Voorhees & Tice, 2000)), and 6 sentence pair datasets (MNLI (Williams et al., 2018), SNLI (Bowman et al., 2015), QNLI (Rajpurkar et al., 2016), RTE (Dagan et al., 2005; Bar Haim et al., 2006; Giampiccolo et al., 2007; Bentivogli et al., 2009), MRPC (Dolan & Brockett, 2005) and QQP⁶). Our datasets represent 6/8 datasets of the GLUE benchmark Wang et al. (2019) (SST-2, MNLI, QNLI, RTE, MRPC, QQP).

In contrast to Gao et al. (2021), we make two modifications to the test sets. First, we split CR into 500 test examples and 3,175 training examples to ensure enough training examples for our 512-shot experiments and secondly, we limit the test sizes to 1,000 examples to speed up kernel evaluations.

⁶<https://www.quora.com/q/quoradata/>

To generate k -shot few-shot datasets, the original training data is used to randomly sample k examples per label for training and another, separate k examples per label for the validation set. Unless otherwise stated, we usually run experiments over 5 seeds of few-shot data sets. We directly use the ‘manual’ prompt templates and label words proposed by Gao et al. (2021), which are reproduced in Table 3. We do include any demonstrations in our prompts.

A.2 COMPUTING THE KERNEL

We use functorch (He & Zou, 2021) to compute the eNTK for RoBERTa-base (125M parameters), using a mix of backward-mode auto-differentiation for computing the jacobians and forward-mode auto-differentiation for computing jacobian-vector products (Novak et al., 2022). Note that $\mathcal{K}^{(\text{SignGD})}$ cannot be computed via jacobian-vector products and requires substantially more memory and run-time in practice.

A.3 SOLVING THE KERNEL

In the standard NTK setting, the initial output of the model $f(\cdot; \theta_0)$ contains no information about solving the task, because θ_0 is a random initialization. However, in the prompted FT setting, we expect the pre-trained model to be able to solve the downstream task well even before any fine-tuning occurs (see Table 6). So, we add the pre-trained model’s output to the output from the kernel. Furthermore, we run a grid search over scaling the labels in order to take advantage of any pre-existing knowledge the model has about the downstream task. In particular, the kernel regression is based on the ℓ_2 distance to the ground truth one-hot vector, but the pre-trained model outputs the logits which will be used for cross-entropy loss. Scaling the one-hot vector by f_0 helps align its scaling with the logits. Our hyperparameter grid for f_0 can be found in Table 4, where ∞ corresponds to not using the pre-trained model logits when solving the kernel.

Solving Multi-Class Tasks There are several options for how to solve C -way classification tasks ($C > 2$). We perform the most general one, which scales with C^2 . Each logit is treated as an independent output of the network, essentially scaling the size N of the original dataset by a factor of C . With CN examples, the kernel now has shape $CN \times CN$. The labels are also scaled up to treat the multi-class problem as many binary classification problems. Solving the multi-class task this way allows the kernel regression model to view relationships between different logits.

Symmetric Kernel Given a symmetric kernel $\mathcal{K} \in \mathbb{R}^{N \times N}$, we solve the kernel regression problem. In particular, we use the representer theorem to write that the empirical risk minimizer of the loss can be expressed as a linear combination of the kernel features computed on the train set.

$$h^*(\cdot) = \arg \min_{h \in \mathcal{H}_{\mathcal{K}}} \frac{1}{N} \sum_{i=1}^N \ell(h(x_i), y_i) \quad \leftrightarrow \quad h^*(\cdot) = \sum_{i=1}^N \alpha_i \mathcal{K}(\cdot, x_i)$$

for a given loss function ℓ . The symmetric SignGD and SGD kernels train α_i via gradient descent to minimize a regularized logistic loss on the downstream task. We search over a grid of regularization strengths chosen proportional to $\|\mathcal{K}\|_{\text{op}}$, see Table 4. For a test input x , the kernel outputs the prediction $h(x) = \sum_i \alpha_i \mathcal{K}(x, x_i)$.

Asymmetric Kernel We write how to solve the kernel regression problem with an asymmetric kernel, developed in He et al. (2022), here. Consider the augmented linear system:

$$\begin{bmatrix} I/\gamma & H \\ H^\top & I/\gamma \end{bmatrix} \begin{bmatrix} \alpha \\ \beta \end{bmatrix} = \begin{bmatrix} 1 \\ 1 \end{bmatrix}$$

where $H_{ij} = y_i \phi_s(x_i)^\top \phi_t(x_j) y_j$ with ϕ_s and ϕ_t as the two different feature maps and y_i as the label for the i th example. In our setting, ϕ_s is the gradient of the datapoint, and ϕ_t is the sign of the gradient. Define ω^* and ν^* as

$$\begin{aligned} \omega^* &= \sum_i \beta_i^* y_i \phi_t(x_i) \\ \nu^* &= \sum_i \alpha_i^* y_i \phi_s(x_i) \end{aligned}$$

Solving this system yields two discriminant functions:

$$\begin{aligned} f_s(x) &= K(x, X)(\beta^* \odot Y) \\ f_t(x) &= K(X, x)(\alpha^* \odot Y) \end{aligned}$$

where $K(x_i, x_j) = \langle \phi_s(x_i), \phi_t(x_j) \rangle$.

We can thus create one discriminant function as $cf_s(x) + (1 - c)f_t(x)$ where $c \in [0, 1]$ is some hyperparameter. When $\phi_s = \phi_t$, we see that $f_s = f_t$ and we reduce to the standard kernel problem (though with repeated equations). Note that per [He et al. \(2022\)](#), this system is only meaningful in terms of stationary points when training α and β using the least squares loss.

We now leverage some specific knowledge about the NTK setting. In particular, we know that we should only use f_s as the predictor in order to correctly represent a new test input in the kernel analog for SignGD.

Experiment	Hyperparameters	Values
SGD FT	Batch size	$\{2, 4, 8\} \times$
	Learning rate	$\{1e-4, 5e-4, 1e-3, 5e-3, 1e-2\}$
SGD-LoRA FT	Batch size	$\{4, 16\} \times$
	Learning rate	$\{1e-4, 1e-3, 1e-2\} \times$
	$(r_{LoRA}, \alpha_{LoRA})$	$\{(8, 16)\}$
Adam FT	Batch size	$\{2, 4, 8\} \times$
	Learning rate	$\{1e-5, 2e-5, 5e-5\}$
Adam-LoRA FT	Batch size	$\{4, 16\} \times$
	Learning rate	$\{1e-5, 4e-5, 4e-4\}$
	$(r_{LoRA}, \alpha_{LoRA})$	$\{(8, 16)\}$
$\mathcal{K}^{(SGD)}, \mathcal{K}^{(SignGD)}$	Kernel regularization	$\{0, 0.001, 0.01, 0.1, 1\} \times$
	f_0 scaling	$\{10, 100, 1000, 10000, \infty\}$
$\mathcal{K}^{(A-SignGD)}$	Kernel regularization	$\{0, 0.001, 0.01, 0.1, 1\} \times$
	f_0 scaling	$\{10, 100, 1000, 10000, \infty\} \times$
	Kernel γ	$\{0.01, 0.1, 1, 10\} \times$
	Kernel c	$\{1\}$

Table 4: The hyperparameter grids used in our experiments.

Hyperparameters and Implementation We follow [Gao et al. \(2021\)](#) in using the few-shot validation set to search over hyperparameters and finding the best hyperparameter per few-shot dataset. We use value ranges given by [Gao et al. \(2021\)](#) and [Hu et al. \(2021\)](#), and search over a wider range of values for SGD. Table 4 shows the hyperparameter grids for fine-tuning and the kernel method.

[Gao et al. \(2021\)](#) train for 1000 steps in the 16-shot setting, and validate the performance every 100 steps to take the best checkpoints. As we consider varying values of k , we use the formula of training for $32kC$ steps and validating every $4kC$ steps, where C is the number of classes in the dataset. This gives a comparable number of training and validation steps for binary tasks in the 16-shot setting.

B ADDITIONAL EXPERIMENTAL RESULTS

Tables 5 and 6 contain the results corresponding to Figures 1 and 2 respectively, and also report results for $k = 64$. Table 7 gives an alternative kernel measurement corresponding to Definition 3.1 and Table 8 supports our explanation of LoRA fine-tuning (Theorem 6.3).

C ROBUSTNESS TO CHOICE OF PROMPT

We explore different choices of prompt and label words in Table 9. When using the results of the prompt and label search from [Gao et al. \(2021\)](#), we find that the kernel approximation matches fine-tuning well. However, the choice of prompt does matter and $\mathcal{K}^{(SGD)}$ performs poorly with the minimal “null prompts” from [Logan IV et al. \(2022\)](#) on sentiment classification datasets, where the prompt is merely “ $\langle S_1 \rangle$ [MASK]” and the label words remain {great, terrible}. We hypothesize this failure is because the task is no longer solvable in the infinite width limit (Definition 7.1).

k -shot	Prompt	Method	SST-2	MR	CR	QNLI	QQP	RTE
16	Prompt	Adam-FT	88.3 _(1.2)	81.3 _(6.1)	93.0 _(1.6)	63.1 _(3.5)	61.8 _(4.5)	57.6 _(6.3)
		SGD-FT	89.0 _(1.5)	83.2 _(2.4)	93.3 _(0.2)	62.1 _(3.1)	62.1 _(2.3)	60.0 _(5.5)
		Kernel SGD	88.3 _(0.3)	84.7 _(1.5)	93.2 _(0.9)	60.1 _(3.3)	58.2 _(0.9)	60.0 _(4.7)
	Standard	Adam-FT	78.1 _(4.2)	69.0 _(6.0)	83.9 _(5.2)	56.7 _(3.6)	58.5 _(5.6)	51.1 _(3.8)
		SGD-FT	77.6 _(4.3)	64.8 _(5.2)	86.6 _(2.6)	51.6 _(1.8)	57.0 _(4.6)	50.2 _(2.1)
		Kernel SGD	62.3 _(6.4)	61.2 _(4.0)	67.5 _(2.3)	50.3 _(1.4)	50.8 _(5.0)	48.7 _(2.0)
64	Prompt	Adam-FT	89.3 _(0.7)	86.0 _(0.4)	93.7 _(0.8)	74.2 _(3.2)	69.8 _(0.6)	67.3 _(2.7)
		SGD-FT	89.7 _(0.4)	85.6 _(1.1)	94.3 _(0.5)	72.8 _(2.2)	69.2 _(1.3)	68.9 _(2.5)
		Kernel SGD	89.2 _(1.0)	86.4 _(0.6)	93.7 _(0.4)	67.3 _(1.6)	66.4 _(1.7)	66.5 _(2.5)
	Standard	Adam-FT	86.1 _(1.2)	83.9 _(1.9)	92.6 _(1.0)	71.5 _(4.5)	65.0 _(3.6)	53.9 _(4.2)
		SGD-FT	85.6 _(1.9)	83.4 _(1.7)	92.6 _(1.1)	65.8 _(4.2)	64.5 _(3.7)	53.6 _(2.5)
		Kernel SGD	77.7 _(2.8)	73.6 _(2.0)	82.6 _(4.4)	54.4 _(1.5)	48.4 _(19.3)	50.0 _(4.4)
512	Prompt	Adam-FT	90.7 _(1.2)	88.6 _(0.6)	94.8 _(0.3)	82.6 _(1.2)	75.7 _(0.9)	75.4 _(3.0)
		SGD-FT	91.8 _(0.4)	89.0 _(0.6)	94.6 _(0.6)	82.5 _(0.5)	76.0 _(1.0)	76.1 _(1.2)
		Kernel SGD	90.2 _(0.4)	88.2 _(0.5)	94.3 _(0.2)	75.1 _(0.7)	70.7 _(1.7)	71.4 _(2.0)
	Standard	Adam-FT	91.4 _(0.7)	88.4 _(0.8)	94.1 _(0.6)	82.2 _(0.3)	76.1 _(0.8)	72.6 _(1.9)
		SGD-FT	91.0 _(0.4)	88.7 _(0.5)	95.6 _(0.4)	81.6 _(1.5)	75.8 _(0.6)	72.0 _(2.2)
		Kernel SGD	84.9 _(2.3)	83.0 _(1.3)	92.1 _(0.7)	68.0 _(1.2)	68.9 _(1.1)	56.5 _(3.1)

Table 5: Fine-tuning performance in the standard FT setting, where the contextual embedding of the [CLS] token is used for classification, and the prompt-based FT setting, where a prompt is added and the embedding for the [MASK] token is used (see Section 3). In standard FT, we initialize the new classification head (i.e., Γ) using the linear probing solution. This table gives the figures in Figure 1, and also relates SGD fine-tuning performance to the more common fine-tuning with Adam.

k -shot	SST-2		MR		CR	
	Lin.	FT	Lin.	FT	Lin.	FT
0	— 79.0 —		— 71.9 —		— 86.2 —	
16	87.5 _(1.3)	88.3 _(1.2)	84.3 _(1.8)	81.3 _(6.1)	93.3 _(0.6)	93.0 _(1.6)
64	88.6 _(0.4)	89.3 _(0.7)	85.0 _(0.2)	86.0 _(0.4)	94.0 _(0.5)	93.7 _(0.8)
512	89.2 _(0.5)	90.7 _(1.2)	86.3 _(0.8)	88.6 _(0.6)	94.0 _(0.5)	93.7 _(0.8)
k -shot	MQPA		Subj		TREC	
	Lin.	FT	Lin.	FT	Lin.	FT
0	— 68.2 —		— 54.6 —		— 27.4 —	
16	75.6 _(3.1)	82.8 _(2.2)	82.9 _(4.7)	87.4 _(2.1)	30.4 _(7.2)	79.6 _(6.1)
64	75.6 _(2.3)	85.0 _(0.2)	78.9 _(14.0)	92.7 _(0.6)	31.2 _(13.0)	92.6 _(1.3)
512	72.1 _(2.2)	87.7 _(0.8)	88.5 _(3.8)	94.8 _(0.5)	35.4 _(12.5)	97.1 _(0.3)
k -shot	MNLI		SNLI		QNLI	
	Lin.	FT	Lin.	FT	Lin.	FT
0	— 48.1 —		— 49.8 —		— 51.2 —	
16	43.6 _(6.4)	56.8 _(2.9)	47.2 _(9.3)	64.6 _(4.1)	57.5 _(2.3)	63.1 _(3.5)
64	55.1 _(4.8)	67.9 _(1.0)	56.9 _(5.7)	76.9 _(1.4)	60.4 _(5.3)	74.2 _(3.2)
512	55.1 _(5.1)	77.9 _(0.8)	55.3 _(6.1)	83.5 _(0.3)	67.7 _(2.0)	82.6 _(1.2)
k -shot	RTE		MRPC		QQP	
	Lin.	FT	Lin.	FT	Lin.	FT
0	— 53.1 —		— 41.7 —		— 42.7 —	
16	55.4 _(6.7)	57.6 _(6.3)	57.7 _(11.6)	68.9 _(2.4)	57.5 _(10.3)	61.7 _(6.5)
64	59.6 _(2.9)	67.3 _(2.7)	64.2 _(2.2)	73.8 _(1.7)	61.7 _(9.4)	72.7 _(1.8)
512	55.5 _(5.6)	75.4 _(3.0)	57.9 _(6.4)	84.8 _(0.8)	66.4 _(1.5)	78.7 _(0.8)

Table 6: Accuracies of pre-trained model (0-shot), linearized model (Lin., see Definition 3.1) and fine-tuned model (FT). Tasks that exhibit the Linearization property of kernel behavior (Definition 3.1) during fine-tuning will show that Lin. performance recovers a substantial amount of the gain in performance achieved by performing fine-tuning. Accuracies are averaged across 5 fine-tuning seeds for each value of k and measured on the test set. This table corresponds to the bar chart in Figure 2.

k -shot	SST-2	MR	CR	MPQA	Subj	trec
16	0.44 _(0.14)	0.41 _(0.13)	0.43 _(0.16)	0.41 _(0.08)	0.43 _(0.28)	2.02 _(0.85)
64	0.41 _(0.07)	0.45 _(0.22)	0.52 _(0.08)	0.42 _(0.13)	0.60 _(0.17)	1.59 _(0.23)
k -shot	MNLI	SNLI	QNLI	RTE	MRPC	QQP
16	0.67 _(0.16)	0.66 _(0.07)	0.48 _(0.10)	0.59 _(0.22)	0.63 _(0.21)	0.46 _(0.10)
64	0.86 _(0.16)	0.65 _(0.03)	0.58 _(0.12)	0.57 _(0.06)	0.86 _(0.08)	0.56 _(0.10)

Table 7: Average element-wise relative distance of $\mathcal{K}^{(\text{SGD})}$ computed on the pre-trained and best fine-tuned model. A smaller value indicates a higher likelihood that the Fixed Features property of kernel behavior (Definition 3.1) holds when performing fine-tuning. Distances are averaged across 5 seeds for each value of k and measured on the LM-BFF test set (Gao et al., 2021).

k -shot	Method	SST-2	MR	CR	QNLI	QQP	RTE
16	SGD-FT	89.0 _(1.5)	83.2 _(2.4)	93.3 _(0.2)	62.1 _(3.1)	62.1 _(2.3)	60.0 _(5.5)
	SGD-LoRA FT	89.1 _(0.6)	82.7 _(2.0)	92.6 _(0.8)	57.1 _(3.3)	59.8 _(3.0)	58.2 _(2.9)
	$\mathcal{K}^{(\text{SGD})}$	88.3 _(0.3)	84.7 _(1.5)	93.2 _(0.9)	60.1 _(3.3)	58.2 _(0.9)	60.0 _(4.7)
	$\mathcal{K}_{\text{LoRA}}^{(\text{SGD})}$	88.1 _(0.4)	84.9 _(1.4)	93.1 _(1.0)	59.4 _(3.7)	58.2 _(3.2)	56.2 _(5.8)
64	SGD-FT	89.7 _(0.4)	85.6 _(1.1)	94.3 _(0.5)	72.8 _(2.2)	69.2 _(1.3)	68.9 _(2.5)
	SGD-LoRA FT	90.0 _(0.2)	85.7 _(1.2)	93.9 _(0.7)	73.8 _(2.7)	68.3 _(2.4)	69.1 _(1.8)
	$\mathcal{K}^{(\text{SGD})}$	89.2 _(1.0)	86.4 _(0.6)	93.7 _(0.4)	67.3 _(1.6)	66.4 _(1.7)	66.5 _(2.5)
	$\mathcal{K}_{\text{LoRA}}^{(\text{SGD})}$	89.2 _(0.7)	85.7 _(1.5)	93.6 _(0.4)	66.0 _(1.6)	63.9 _(4.5)	63.5 _(3.5)

Table 8: Performance of prompt-based SGD FT and prompt-based SGD-LoRA FT, along with their kernel analogs $\mathcal{K}^{(\text{SGD})}$ and $\mathcal{K}_{\text{LoRA}}^{(\text{SGD})}$, on a subset of tasks. SGD FT and SGD-LoRA FT achieve comparable performance, and $\mathcal{K}^{(\text{SGD})}$ and $\mathcal{K}_{\text{LoRA}}^{(\text{SGD})}$ also achieve comparable performance to each other. We report F1 for QQP and accuracy otherwise, and average the metrics over 5 seeds. These experiments support Theorem 6.3.

k -shot	Prompt + label format	Method	SST-2	MR	CR	QNLI	QQP	RTE
16	Manual (Gao et al., 2021)	Adam-FT	88.3 _(1.2)	81.3 _(6.1)	93.0 _(1.6)	63.1 _(3.5)	61.8 _(4.5)	57.6 _(6.3)
		SGD-FT	89.0 _(1.5)	83.2 _(2.4)	93.3 _(0.2)	62.1 _(3.1)	62.1 _(2.3)	60.0 _(5.5)
		$\mathcal{K}^{(\text{SGD})}$	88.3 _(0.3)	84.7 _(1.5)	93.2 _(0.9)	60.1 _(3.3)	58.2 _(0.9)	60.0 _(4.7)
Prompt + label search (Gao et al., 2021)	Adam-FT	88.1 _(0.8)	81.6 _(3.8)	92.8 _(0.4)	56.3 _(3.8)	58.6 _(4.5)	58.6 _(4.6)	
	SGD-FT	89.2 _(1.2)	80.1 _(1.8)	93.2 _(0.5)	58.7 _(4.8)	59.0 _(1.4)	61.6 _(2.6)	
	$\mathcal{K}^{(\text{SGD})}$	88.6 _(1.1)	78.5 _(1.2)	93.5 _(0.7)	56.7 _(1.7)	60.2 _(2.0)	57.4 _(5.5)	
Null prompts (Logan IV et al., 2022)	Adam-FT	87.6 _(0.9)	82.6 _(0.6)	92.8 _(0.6)	59.0 _(2.9)	57.5 _(5.2)	56.4 _(4.7)	
	SGD-FT	88.1 _(0.7)	82.8 _(3.6)	93.4 _(0.7)	59.0 _(3.4)	57.6 _(5.5)	54.1 _(1.6)	
	$\mathcal{K}^{(\text{SGD})}$	78.3 _(4.3)	78.7 _(1.8)	91.7 _(0.8)	55.8 _(2.7)	57.4 _(1.8)	55.5 _(2.3)	

Table 9: We experiment with different prompt formats and label words: using the top result of an automatic prompt search performed on RoBERTa-large (Table E.1 in Gao et al. (2021)); and minimal null prompts (Table A3, Logan IV et al. (2022)), which add no additional text to the prompt. We find that our observations are robust to the choice of prompt, with the exception of the more unnatural “null prompts” on sentiment tasks (SST-2, MR, CR), which show a substantial gap between $\mathcal{K}^{(\text{SGD})}$ and fine-tuning. We report F1 for QQP and accuracy otherwise, and average the metrics over 5 seeds.

D KERNEL BEHAVIOR AND THE PARAMETRIZATION

Neural network training can exhibit either kernel behavior or feature learning behavior. These were described in [Woodworth et al. \(2020\)](#) as the lazy regime and active regime, respectively, when training from a random initialization. Kernel behavior provides a tractable tool to study the training of neural networks, but it is not believed to be a complete description of practical deep learning settings. In particular, kernel behavior implies the feature (i.e., gradient) of the neural networks remains unchanged in the overparameterized setting, which is not true in practical pre-training of large models.

[Yang & Hu \(2021\)](#) showed how the initialization variance, multiplier, and learning rate for each parameter can move training from the kernel behavior to the feature learning behavior. They further developed the Maximal Update Parametrization (abbreviated MUP or μP) where every parameter is updated maximally (in terms of scaling with width) while keeping the network stable. [Yang et al. \(2022\)](#) then extends μP to Transformers with Adam optimization, and showed empirically that for pre-training of large language models using μP , the optimal hyperparameters remain the same when increasing width. It allows more comprehensive hyperparameter searches on a smaller model and direct transfer of the resulting optimal hyperparameters to the larger model, resulting in markedly improved pre-training performance.

This section discusses two of our formal results: Theorems 4.3 and 7.3. In general, we consider the overparameterized setting in which the width of the network goes to infinity. Additionally, we assume that when initializing a weight matrix of the model, each entry of the matrix is drawn from i.i.d. Gaussian distribution. In particular, we model a pre-trained model as a non-random initialization that arose from training starting at a random initialization. We use Tensor Programs ([Yang, 2020b](#)) for our formal results.

This section is organized as follows. In Appendix D.1, we introduce the basic notation and ideas around Tensor Programs as well as the assumptions we need to make in order for an infinite-width limit to be interesting to study. Then, Appendix D.2 gives the formal proof for the kernel analog to SignGD (Theorem 4.3). In Appendix D.3, we provide a formal proof of how fine-tuning can exhibit kernel behavior (Theorem 7.3). The proof relies heavily on Tensor Programs, so we additionally provide a more accessible and intuitive sketch on linear networks in Appendix D.5. Finally, in Appendix D.6, we show that standard FT can exhibit kernel behavior when studying the infinite-width limit, though experiments in Table 5 suggest otherwise. This contradiction between theory and practice suggests that realistic finite-width networks are too far from infinite width ones when performing standard FT. Nevertheless, wider models may exhibit kernel behavior when performing standard FT.

D.1 PRELIMINARIES

Notations Let $\xi \in \mathbb{R}^{d_{in}}$ be the input of the network. Let n be the hidden dimension of the network and d_{out} be the output dimension of the network. We define the network as a function of the following form:

$$f(\xi; \{U^i\}_i, \{W^j\}_j, V) = V^\top h(\xi; \{U^i\}_i, \{W^j\}_j),$$

where ξ is the input, $U^i \in \mathbb{R}^{n \times d_{in}}$ are the input weight matrices, $W^j \in \mathbb{R}^{n \times n}$ are hidden weight matrices, $V \in \mathbb{R}^{n \times d_{out}}$ is the output weight matrix, and $h(\xi; \{U^i\}_i, \{W^j\}_j) \in \mathbb{R}^n$ is the input of last layer (readout layer).⁷ We write \mathcal{M} as the set of weight matrices, i.e., $\mathcal{M} = \{U^i\}_i \cup \{W^j\}_j \cup \{V\}$. For $M \in \mathcal{M}$, let $\nabla_M f(\xi)$ be the gradient of f w.r.t. M at input ξ .

To simplify the notation, we assume $d_{in} = 1$ in this section. We will note when an extension to $d_{in} > 1$ requires a non-trivial step. For any weight matrix $M \in \mathcal{M}$, let γ_M be the multiplier of M , such that M is multiplied by γ_M before performing matrix multiplication. Let η_M be the learning rate of the weight M . Let σ_M^2 be the variance of entries of M at initialization, so each entry of M is drawn $\mathcal{N}(0, \sigma_M^2)$ independently.

Because we are considering the infinite-width limit, $f(\xi; \{U^i\}_i, \{W^j\}_j, V)$ actually represents a series of increasingly wide networks $\{f^n(\xi; \{U^{i,n}\}_i, \{W^{j,n}\}_j, V^n)\}_{n>0}$ of the same architecture,

⁷We are able to describe transformers (without weight tying) in the definition. The bias can be regarded as input weights assuming there is a coordinate in ξ that is always 1.

but f^n has a hidden dimension n . We use the notation f to describe the model architecture, the training optimizer of the model, and $\gamma_M, \eta_M, \sigma_M$ for every weight matrix M in the model.

Let M_t be the weight matrix at time step t of training. If the network is pre-trained, we let M_{-1} be the weight matrix before pre-training, and M_0 be the parameters right after pre-training. Let $\Delta M_t = M_t - M_{t-1}$ be the change each training step induces. Let f_t be the network at step t that

$$f_t(\xi) = f(\xi; \{U_t^i\}_i, \{W_t^j\}_j, V_t).$$

Let ξ_t, y_t be the training input and target at step t , and let the loss function at step t be $\mathcal{L}_t(f_t(\xi_t)) = \mathcal{L}(f_t(\xi_t), y_t)$. Let $\chi_t = \mathcal{L}'_t(f_t(\xi_t))$ be the derivative of the loss function.

Big-O Notation For a series of scalar random variables $c = \{c^n\}_{n>0}$ and a function $e : \mathbb{N} \rightarrow \mathbb{R}$, we say $c = \Theta(e(n))$ if there exist A, B such that for sufficiently large n , $|c^n| \in [Ae(n), Be(n)]$ almost surely. For a series of vector random variables $x = \{x^n\}_{n>0}$, we say that x is coordinate-wise $\Theta(n^a)$, or $x = \Theta(e(n))$ if this series of scalar random variables $\{\|x^n\|_2/\sqrt{n}\}_{n>0}$ is $\Theta(e(n))$. Similarly for the notation $O(e(n))$, $\Omega(e(n))$, and $o(e(n))$. For convenience, we assume every $e(n)$ in this section is equal to n^a for some a .

Tensor Programs We refer reader to see Section 7 of [Yang & Hu \(2021\)](#) for detailed explanation and full definition of Tensor Programs. Here, we provide a simple overview of Tensor Programs:

Definition D.1 (Definition 7.1 of [Yang & Hu \(2021\)](#)). A Tensor Program is a sequence of \mathbb{R}^n -vectors and \mathbb{R} -scalars inductively generated via one of the following ways from an initial set \mathcal{C} of random scalars, \mathcal{V} of random \mathbb{R}^n vectors, and a set \mathcal{W} of random $\mathbb{R}^{n \times n}$ matrices.

MatMul Given $W \in \mathbb{R}^{n \times n}$ and $x \in \mathbb{R}^n$, we can generate $Wx \in \mathbb{R}^n$ or $W^\top x \in \mathbb{R}^n$.

Nonlin Given $\phi : \mathbb{R}^k \times \mathbb{R}^l \rightarrow \mathbb{R}$, previous scalar $\theta_1, \dots, \theta_l \in \mathbb{R}$ and vector $x^1, \dots, x^k \in \mathbb{R}^n$, we can generate a new vector

$$\phi(x^1, \dots, x^k; \theta_1, \dots, \theta_l) \in \mathbb{R}^n$$

where $\phi(-; \theta_1, \dots, \theta_l)$ applies coordinate-wise to each “ α -slice” $(x_\alpha^1, \dots, x_\alpha^k)$.

Moment Given the same setup as above, we can also generate a new scalar

$$\frac{1}{n} \sum_{\alpha=1}^n \phi(x_\alpha^1, \dots, x_\alpha^k; \theta_1, \dots, \theta_l) \in \mathbb{R}.$$

[Yang \(2019; 2020a\)](#); [Yang & Littwin \(2021\)](#); [Yang et al. \(2022\)](#) show that Tensor Programs can express the computation, SGD/Adam optimization, and the kernel of almost any general architecture.

The key result of the Tensor Programs is that we can represent the coordinates of any vector x in the Tensor Program with a random variable Z^x , and represent any scalar θ with a deterministic scalar $\hat{\theta}$. There is a way to define all $\hat{\theta}$ and Z^x correspond to the Tensor Program (cf. Definition 7.3 in [Yang & Hu \(2021\)](#)), and the Master Theorem of the Tensor Program shows that $\theta \rightarrow \hat{\theta}$ when $n \rightarrow \infty$ (cf. Theorem 7.4 in [Yang & Hu \(2021\)](#)).

Although it is in general hard to compute Z^x and $\hat{\theta}$, it allows us to reason about the scales of vectors in the training of a network.

Assumptions Related to Tensor Programs. Since we are studying the infinite width limit and using Tensor Programs as our framework, there are some mild assumptions that we need in order to apply Tensor Programs and results in [Yang & Hu \(2021\)](#).

Assumption D.2. We assume the network f satisfies the following

- a) The forward pass of f in the infinite-width limit can be written as Tensor Programs.
- b) The hidden vectors have $\Theta(1)$ coordinates at initialization.
- c) The hidden vectors have $O(1)$ coordinates during training.

- d) For any training scheme⁸ and any constant t and any input ξ , $f_t(\xi) = O(1)$.
- e) There exist a training scheme and some constant t and input ξ such that $f_t(\xi) - f_0(\xi) = \Theta(1)$.
- f) The activation function of f is tanh or σ -gelu for a small enough σ (so it approximates ReLU), where

$$\sigma\text{-gelu}(x) = \frac{1}{2}x\text{erf}(\sigma^{-1}x) + \sigma\frac{e^{-\sigma^{-2}x^2}}{2\sqrt{\pi}} + \frac{x}{2}.$$

Furthermore, we have one assumption on SignGD:

- g) SignGD is approximated as the sign function being replaced with ϵ -sign for small enough ϵ when updating parameters, where $\epsilon\text{-sign}(x) = \frac{x}{|x|+\epsilon}$ is smoothed version of sign. We assume using different ϵ when computing the sign of $\nabla_M f$, so that ϵ for $\nabla_M f$ match the maximum scale of $\nabla_M f$.

b), c), d) and e) in Assumption D.2 together recover the definition of nontrivial stable network in Yang & Hu (2021). b) and c) ensure that the pre-activations in the network are not too large, so that activation functions (e.g., tanh) are not trivialized to always output ± 1 . b) ensures that the pre-activations in the network are not too small at initialization, so the activation function is not trivialized to its first-order Taylor expansion. d) ensures the network output is bounded. e) ensures that the network is not frozen during training (i.e., learning can occur).

f) and g) in Assumption D.2 assures all non-linear functions that appear in the Tensor Programs is pseudo-Lipschitz, which is required for the Master Theorem of Tensor Programs. g) also assures that ϵ -sign is not trivialize to 0 or sign when $\nabla_M f \neq \Theta(1)$.

D.2 SIGNGD KERNEL DERIVATION

Definition D.3 (Formal Definition of Kernel Behavior). We say that this network training process demonstrates *kernel behavior* if the following properties are satisfied.

1. *Linearization*: The change of the network can be approximated by its first order Taylor expansion, i.e.,

$$\lim_{n \rightarrow \infty} \frac{f_t(\xi) - f_{t-1}(\xi)}{\chi_t} = \lim_{n \rightarrow \infty} \sum_{M \in \mathcal{M}} \left\langle \nabla_M f_{t-1}(\xi), \frac{\Delta M_t}{\chi_t} \right\rangle;$$

2. *Fixed Features*: The gradients at step t are approximately the same as before training, i.e.,

$$\forall M \in \mathcal{M}, \lim_{n \rightarrow \infty} \frac{\|\nabla_M f_t(\xi) - \nabla_M f_0(\xi)\|_2^2}{\max_{\xi'} \|\nabla_M f_0(\xi')\|_2^2} = 0.$$

Note that we define Linearization with both LHS and RHS divided by χ_t so it is meaningful for the case of $\chi_t = o(1)$. We do the same thing in the following theorem.

Theorem D.4 (SignGD Kernel). *If SignGD training of f demonstrates kernel behavior, then under Assumption D.2,*

$$\lim_{n \rightarrow \infty} \frac{f_t(\xi) - f_{t-1}(\xi)}{\chi_t} = \lim_{n \rightarrow \infty} \sum_{M \in \{U^i\}_i \cup \{W^j\}_j \cup \{V\}} -\eta_M \langle \nabla_M f_0(\xi), \epsilon\text{-sign}(\nabla_M f_0(\xi_t)) \rangle.$$

Note if $\eta_M = \eta$, the RHS of the equation above equals to

$$-\eta \langle \nabla f_0(\xi), \epsilon\text{-sign}(\nabla f_0(\xi_t)) \rangle \approx -\eta \mathcal{K}^{(\text{A-SignGD})}(\xi, \xi_t),$$

where the approximation comes from the difference between ϵ -sign and sign.

⁸Training scheme means a sequence of training examples $\{(\xi_t, y(\xi_t))\}$, and loss function $\ell(f_t(\xi_t), y(\xi_t))$.

Proof. By the update rule of SignGD, $\frac{\Delta M_t}{\chi_t} = -\eta_M \epsilon\text{-sign}(\nabla_M f_{t-1})$. It suffices to prove

$$\eta_M \langle \nabla_M f_t(\xi), \epsilon\text{-sign}(\nabla_M f_t(\xi_t)) \rangle = \eta_M \langle \nabla_M f_0(\xi), \epsilon\text{-sign}(\nabla_M f_0(\xi_t)) \rangle$$

when $n \rightarrow \infty$.

Since

$$\begin{aligned} & \eta_M \langle \nabla_M f_t(\xi), \epsilon\text{-sign}(\nabla_M f_t(\xi_t)) \rangle - \eta_M \langle \nabla_M f_0(\xi), \epsilon\text{-sign}(\nabla_M f_0(\xi_t)) \rangle \\ &= \eta_M \langle \nabla_M f_t(\xi) - \nabla_M f_0(\xi), \epsilon\text{-sign}(\nabla_M f_t(\xi_t)) \rangle + \end{aligned} \quad (4)$$

$$\eta_M \langle \nabla_M f_t(\xi), \epsilon\text{-sign}(\nabla_M f_t(\xi_t)) - \epsilon\text{-sign}(\nabla_M f_0(\xi_t)) \rangle + \quad (5)$$

$$\eta_M \langle \nabla_M f_t(\xi) - \nabla_M f_0(\xi), \epsilon\text{-sign}(\nabla_M f_t(\xi_t)) - \epsilon\text{-sign}(\nabla_M f_0(\xi_t)) \rangle, \quad (6)$$

we only need to prove Equations (4) to (6) are all 0 when $n \rightarrow \infty$.

Let $\xi^* = \arg \max_{\xi^*} \|\nabla_M f_0(\xi^*)\|_2^2$ be the input of maximum gradient scale, then by Fixed Features, we have

$$\frac{\|\nabla_M f_t(\xi) - \nabla_M f_0(\xi)\|_2}{\|\nabla_M f_0(\xi^*)\|_2} = o(1).$$

Since $\epsilon\text{-sign}(x) - \epsilon\text{-sign}(y) \leq |x - y|/\epsilon$,

$$\|\epsilon\text{-sign}(\nabla_M f_t(\xi)) - \epsilon\text{-sign}(\nabla_M f_0(\xi))\|_2 \leq \|\nabla_M f_t(\xi) - \nabla_M f_0(\xi)\|_2/\epsilon. \quad (7)$$

Combined with $\|\nabla_M f_0(\xi^*)\|_2/\sqrt{N} = \Theta(\epsilon)$ (N is the number of entries of M , this is by **g**) of Assumption D.2), we have

$$\begin{aligned} & \frac{\|\epsilon\text{-sign}(\nabla_M f_t(\xi)) - \epsilon\text{-sign}(\nabla_M f_0(\xi))\|_2}{\|\epsilon\text{-sign}(\nabla_M f_0(\xi^*))\|_2} \\ & \leq \frac{\|\nabla_M f_t(\xi) - \nabla_M f_0(\xi)\|_2/\epsilon}{\|\epsilon\text{-sign}(\nabla_M f_0(\xi^*))\|_2} \quad \text{by eq. (7)} \\ & = \frac{\|\nabla_M f_t(\xi) - \nabla_M f_0(\xi)\|_2}{\|\nabla_M f_0(\xi^*)\|_2} \cdot \frac{\|\nabla_M f_0(\xi^*)\|_2/\sqrt{N}}{\epsilon\|\epsilon\text{-sign}(\nabla_M f_0(\xi^*))\|_2/\sqrt{N}} \\ & = \frac{\|\nabla_M f_t(\xi) - \nabla_M f_0(\xi)\|_2}{\|\nabla_M f_0(\xi^*)\|_2} \cdot \Theta(1) = o(1). \end{aligned}$$

By d) in Assumption D.2, and consider the training scheme that sets $\xi_1 = \xi^*$ and the loss function ℓ so $\chi_1 = \Theta(1)$, then

$$\frac{f_1(\xi^*) - f_0(\xi^*)}{\chi_1} = -\eta_M \langle \nabla_M f_0(\xi^*), \epsilon\text{-sign}(\nabla_M f_0(\xi^*)) \rangle = O(1).$$

And it is easy to see that $\langle \nabla_M f_0(\xi^*), \epsilon\text{-sign}(\nabla_M f_0(\xi^*)) \rangle$ and $\|\nabla_M f_0(\xi^*)\|_2 \|\epsilon\text{-sign}(\nabla_M f_0(\xi^*))\|_2$ has the same scale.

Now it suffices to prove Equations (4) to (6) divided by $\eta_M \|\nabla_M f_0(\xi^*)\|_2 \|\epsilon\text{-sign}(\nabla_M f_0(\xi^*))\|_2$ are all 0 when $n \rightarrow \infty$. For Equation (4),

$$\begin{aligned} & \frac{\eta_M \langle \nabla_M f_t(\xi) - \nabla_M f_0(\xi), \epsilon\text{-sign}(\nabla_M f_t(\xi_t)) \rangle}{\eta_M \|\nabla_M f_0(\xi^*)\|_2 \|\epsilon\text{-sign}(\nabla_M f_0(\xi^*))\|_2} \\ & \leq \frac{\|\nabla_M f_t(\xi) - \nabla_M f_0(\xi)\|_2 \|\epsilon\text{-sign}(\nabla_M f_t(\xi_t))\|_2}{\|\nabla_M f_0(\xi^*)\|_2 \|\epsilon\text{-sign}(\nabla_M f_0(\xi^*))\|_2} \\ & = \frac{\|\nabla_M f_t(\xi) - \nabla_M f_0(\xi)\|_2}{\|\nabla_M f_0(\xi^*)\|_2} = o(1). \end{aligned}$$

Similarly, for Equation (5),

$$\begin{aligned} & \frac{\eta_M \langle \nabla_M f_t(\xi), \epsilon\text{-sign}(\nabla_M f_t(\xi_t)) - \epsilon\text{-sign}(\nabla_M f_0(\xi_t)) \rangle}{\eta_M \|\nabla_M f_0(\xi^*)\|_2 \|\epsilon\text{-sign}(\nabla_M f_0(\xi^*))\|_2} \\ & \leq \frac{\|\epsilon\text{-sign}(\nabla_M f_t(\xi)) - \epsilon\text{-sign}(\nabla_M f_0(\xi))\|_2}{\|\epsilon\text{-sign}(\nabla_M f_0(\xi^*))\|_2} = o(1), \end{aligned}$$

and for Equation (6),

$$\begin{aligned} & \frac{\eta_M \langle \nabla_M f_t(\xi) - \nabla_M f_0(\xi), \epsilon\text{-sign}(\nabla_M f_t(\xi_t)) - \epsilon\text{-sign}(\nabla_M f_0(\xi_t)) \rangle}{\eta_M \|\nabla_M f_0(\xi^*)\|_2 \|\epsilon\text{-sign}(\nabla_M f_0(\xi^*))\|_2} \\ \leq & \frac{\|\epsilon\text{-sign}(\nabla_M f_t(\xi)) - \epsilon\text{-sign}(\nabla_M f_0(\xi))\|_2}{\|\epsilon\text{-sign}(\nabla_M f_0(\xi^*))\|_2} \cdot \frac{\|\nabla_M f_t(\xi) - \nabla_M f_0(\xi)\|_2}{\|\nabla_M f_0(\xi^*)\|_2} = o(1). \end{aligned}$$

□

D.3 PROMPT-BASED FINE-TUNING

Prompt-based fine-tuning uses the pre-trained network directly without substituting or adding any parameters. Therefore, without any additional assumptions, the behaviors of fine-tuning and pre-training are the same from the perspective of the Tensor Programs. We thus adopt the assumption that $\chi_t = o(1)$. Intuitively, this assumption is believable because wider pre-trained networks can solve downstream tasks better. In this section, we prove that prompt-based fine-tuning exhibits kernel behavior when this assumption holds.

Theorem D.5. *If the downstream task is solvable for network f , that is, for any t , $\chi_t = o(1)$, then under Assumption D.2, the fine-tuning of f exhibits kernel behavior (Definition D.3).*

Below we provide a proof that is heavily based on Tensor Programs and the analysis in Yang & Hu (2021). For readers who are not familiar with Tensor Programs, we provide intuitive examples in the next few subsections, where we focus on a three-layer linear network parameterized with μP .

Proof. We first prove the theorem under the assumption that the network is a multilayer perceptron and the optimizer is SGD, which is the same setting as Yang & Hu (2021). We will later extend this to more general cases.

Consider the following L -hidden-layer perceptron:

$$h^1(\xi) = U\xi,$$

and

$$x^l(\xi) = \phi(h^l(\xi)), \quad h^{l+1}(\xi) = W^{l+1}x^l(\xi), \quad \text{for } l = 1, \dots, L-1,$$

and

$$f(\xi) = Vx^L(\xi).$$

Following Yang & Hu (2021), we let the learning rate for every parameter equal to ηn^{-c} . Let $W^1 = U$ and $W^{L+1} = V$, and for $l = 1, \dots, L+1$, we parametrize W^l as $W^l = \gamma_l w^l$ for actual trainable parameter w^l , and we initialize each coordinate w^l i.i.d. from $\mathcal{N}(0, \sigma_l^2)$. The setting covers all parameterizations based on Lemma D.6. For convenience, we assume $\gamma_l = n^{-a_l}$ and $\sigma_l = n^{-b_l}$. Without loss of generality, we further assume that $\chi_t = \Theta(n^{-d})$ (rather than $\chi_t = o(1)$ only).

By Theorem 3.3 of Yang & Hu (2021), stable network implies

$$r \triangleq \min(a_{L+1} + b_{L+1}, 2a_{L+1} + c) + c - 1 + \min_{l=1}^L [2a_l + \mathbb{I}(l=1)] \geq 0.$$

Also by Theorem 3.8 of Yang & Hu (2021), for nontrivial stable network (included in Assumption D.2), if $r > 0$ then there exists a kernel \mathcal{K} such that

$$f_{t+1}(\xi) = f_t(\xi) - \eta \chi_t \mathcal{K}(\xi, \xi_t),$$

which is very close to our definition of kernel behavior. In fact, we will prove that they are equivalent in the fine-tuning case.

Since $\chi_t = \Theta(n^{-d})$ for fine-tuning, it is equivalent to set the learning rate to ηn^{-c-d} and replace χ_t with $\hat{\chi}_t = n^d \chi_t$. Formally, we are considering the following training scheme: at the pre-training stage, $r \geq 0$ (so it could demonstrate feature learning or kernel behavior); at the fine-tuning stage, c is increased to $c' \triangleq c + d > c$, thus, the corresponding r is increased to be strictly greater than 0. Therefore, it suggests kernel behavior with following caveats.

Do we handle the case of different learning rates during pre-training and fine-tuning? The answer is *effectively YES*, because the above scheme is equivalent to training from scratch with learning rate ηn^{c-d} . First of all, the scale of the update on W^l , h^l , x^l and f are all multiplied by n^{-d} when switching from the pre-training stage (ηn^{-c} learning rate) to the fine-tuning stage (ηn^{-c-d} learning rate). The scales are exactly the same as training from scratch with ηn^{-c-d} learning rate except b_{L+1} needs to be changed to $b'_{L+1} \triangleq \min(b_{L+1}, a_{L+1} + c)$. Note this change of b_{L+1} does not affect the fact that r is updated to $r' \triangleq r + d > 0$.

Does $r' > 0$ formally imply our definition of kernel behavior (Definition D.3)? The answer is *YES*. We first prove Fixed Features in Definition D.3. The gradient of matrix W^l is equal to outer product between $\nabla_{h^l} f$ (gradient w.r.t. h^l) and x^{l-1} . Let dh_t^l be the normalized gradient w.r.t. h^l at step t (so $dh_t^l = \Theta(1)$), and x_t^l be the x^l at step t ($x_t^l = \Theta(1)$ without normalization). It suffices to prove $dh_t^l - dh_0^l = O(1)$ and $x_t^l - x_0^l = o(1)$. The later was proved by Proposition H.27 of Yang & Hu (2021). To prove $dh_t^l - dh_0^l = O(1)$, we let dx_t^l be the normalized gradient w.r.t. x^l at step t , and compute the scale of $dh_t^l - dh_{t-1}^l$ and $dx_t^l - dx_{t-1}^l$ inductively from $l = L$ to $l = 1$. We obtain that they both has the same scale of

$$n^{-\min(2a_{L+1}+c-a_{L+1}-b'_{L+1}, a_{L+1}+b_{L+1}+c'-1+\min_{m=l+1}^L 2a_m)} \leq n^{-\min(0, r')} = 1,$$

the inequality is because $b'_{L+1} \leq a_{L+1} + c$ and $r' \leq a_{L+1} + b_{L+1} + c' - 1 + \min_{m=l+1}^L 2a_m$.

Second, we prove Linearization in Definition D.3. We need to first make a very slight modification to the Tensor Program in Yang & Hu (2021), that is, changing the computation of $f_t(\xi) - f_{t-1}(\xi)$ to $n^{-d}(f_t(\xi) - f_{t-1}(\xi))$. By Theorem H.32 of Yang & Hu (2021) and its definition of Σ , we can show that

$$\begin{aligned} \lim_{n \rightarrow \infty} n^{-d}(f_t(\xi) - f_{t-1}(\xi)) &= \lim_{n \rightarrow \infty} \sum_{l=1}^{L+1} \eta n^{-c-d} \langle \nabla_{W^l} f_{t-1}(\xi), \nabla_{W^l} f_{t-1}(\xi_t) \rangle \\ &= \lim_{n \rightarrow \infty} \sum_{l=1}^{L+1} \left\langle \nabla_{W^l} f_{t-1}(\xi), \frac{\Delta W_t^l}{n^{-d}} \right\rangle. \end{aligned}$$

From SGD to SignGD. Since $\text{sign}(xy) = \text{sign}(x) \text{sign}(y)$, the update of matrix W^l can still be written as outer product of two vectors, i.e., $\Delta W_t^l = \eta n^{-c} \chi_t \text{sign}(\nabla_{h^l} f_{t-1}) \otimes \text{sign}(x_{t-1}^{l-1})$. After applying sign , the scale of vector changes. If the parametrization is the same, the scales of vectors using SignGD will be different from those using SGD. This can be easily resolved by changing learning rates for each parameter, so the scaling change brought by sign is corrected. Furthermore, as mentioned in Assumption D.2, we need to approximate sign by a smoothed version ϵ - sign so the Master Theorem of Tensor Programs can still apply.

Extension to universal architectures. The theorem is correct for any network whose first forward pass can be written as Tensor Programs. Given this condition, the forward pass, backward pass, and kernel of any step can be written as Tensor Programs (Yang, 2020a;b). To analyse the scaling of the Tensor Program will need the following steps:

1. *Extension to general computation graph.* We can still inductive reason about the scale of preactivations and activations by the topological order of the computation graph; and similarly reason about the gradient by the reverse topological order.
2. *Extension to weight sharing.* We may use weights multiple times in a forward pass. The preactivations, activations and their gradients will not be affected. Only the update of a weight is now sum of several vector outer product depending on the number of occurrence of the weight.

□

D.4 MUP FOR SGD AND SIGNGD

In the following subsections, we provide more intuition for Theorem D.5. Although we consider all types of pre-trained models, we are mostly interested in models with feature learning behavior,

because it is likely not true that gradients can be approximated as fixed throughout the entirety of *pre-training*. For pre-trained models with kernel behavior, it is obvious that fine-tuning with the same settings as pre-training (i.e., prompt-based FT) will also exhibit kernel behavior. Furthermore, Theorem H.17 of Yang & Hu (2021) proved that if the last layer is replaced with a freshly initialized layer (i.e., standard FT), fine-tuning from a pre-trained models with kernel behavior is the same as training on the downstream task from scratch.

Among all the pre-training schemes that exhibit feature learning behavior, μP is special because each parameter (except the last layer) can *on its own* push the model to perform feature learning. Therefore, to build an intuitive description of fine-tuning behavior, we assume that the model was pre-trained by μP . We note again that our main result *does not require* this assumption.

The formulation of μP contains three sets of hyperparameters: initial variance of M , multiplier of M and learning rate of M for $M \in \{U^i\}_i \cup \{W^j\}_j \cup \{V\}$. However, even if we restrict these three hyperparameters to be in the form of n^α , μP is not unique, because there is one degree of freedom for each weight according to the following lemma.

Lemma D.6 (Lemma J.1 of Yang et al. (2022)). *Consider a weight matrix M with learning rate C , initialized as $M \sim \mathcal{N}(0, B^2)$, and with a multiplier A . Then for any $\gamma > 0$, $f_t(\xi)$ stays fixed for all t and ξ if we set*

- $A \leftarrow A\gamma, B \leftarrow B/\gamma, C \leftarrow C/\gamma^2$ if training with SGD.
- $A \leftarrow A\gamma, B \leftarrow B/\gamma, C \leftarrow C/\gamma$ if training with Adam.

Note the conclusion about Adam in Lemma D.6 also extends to SignGD.

With Lemma D.6, we can always set the multiplier of any weight matrix M to be 1, which leave us only the initialization variance σ_M^2 and learning rate η_M . Furthermore, in terms of the scale at initialization and the scale of updates, μP for SGD and SignGD are entirely the same. The only difference would be learning rate. We provide details in Table 10 (recall M_{-1} is the weight M at initialization of pre-training, $\Delta M_0 = M_0 - M_{-1}$ is the overall change of weight in pre-training).

coordinate-wise scale	$M = U^i$	$M = W^j$	$M = V$
M_{-1}	$\Theta(1)$	$\Theta(1/\sqrt{n})$	$\Theta(1/n)$
ΔM_0	$\Theta(1)$	$\Theta(1/n)$	$\Theta(1/n)$
η_M for SGD	$\Theta(n)$	$\Theta(1)$	$\Theta(1/n)$
η_M for signGD/Adam	$\Theta(1)$	$\Theta(1/n)$	$\Theta(1/n)$

Table 10: Scales of initialization, update and learning rate for μP in pre-training.

Since we have different learning rate for η_M , the kernel that we care is defined as

$$\mathcal{K}(\xi, \xi') = \sum_{M \in \mathcal{M}} \eta_M \langle \nabla_W f(\xi), \phi(\nabla_W f(\xi')) \rangle,$$

where ϕ is identity if the algorithm is SGD, $\phi = \text{sign}$ if the algorithm is SignGD. And we want to prove the dynamic of the network follows

$$\frac{f_t(\xi) - f_{t-1}(\xi)}{\chi_t} \rightarrow -\mathcal{K}(\xi, \xi_t) \quad \text{when } n \rightarrow \infty.$$

D.5 PROMPT-BASED FINE-TUNING: A LINEAR EXAMPLE

As an intuitive example, we consider a three-layer linear network

$$f(\xi; U, W, V) = V^\top W U \xi.$$

For simplicity, we train the network with SGD, and freeze V so $\eta_V = 0$. Then we have $\nabla_U f = W^\top V \xi^\top$ and $\nabla_W f = V(U \xi)^\top$. We assume $|\langle \xi, \xi' \rangle| > 0$ for any ξ, ξ' .

In what follows, we will prove that for pre-training f cannot be written as the first-order Taylor expansion (i.e., it exhibits feature learning). Then we will prove that it is the opposite for

fine-tuning. In fact, if we only look at one gradient step, the only higher order term equals to $\eta_W \eta_U \chi_t^2 \|V\|^2 \langle \xi_t, \xi \rangle f_{t-1}(\xi) = \Theta(\chi_t^2 f_{t-1}(\xi))$, where $f_{t-1}(\xi)$ is mostly $\Theta(1)$, χ_t is mostly $\Theta(1)$ in pre-training⁹ and $o(1)$ in fine-tuning (by Definition 7.1).

Zero step (Pre-training) We model the pre-training of f as one step of training with $\chi_0 = \Theta(1)$. Then we have $\Delta U_0 = -\eta_U \chi_0 W_{-1}^\top V \xi_0^\top$, and $\Delta W_0 = -\eta_W \chi_0 V (U_{-1} \xi_0)^\top$. Since W_{-1}^\top is independent from V , we have $W_{-1}^\top V = \Theta(1/n)$, thus $\Delta U_0 = \Theta(1)$ matching Table 10. On the other hand, it is obvious that $\Delta W_0 = \Theta(1/n)$ because $V = \Theta(1/n)$ and $U = \Theta(1)$, also matching Table 10.

Then the function is now

$$\begin{aligned} f_0(\xi) &= V^\top (W_{-1} + \Delta W_0)(U_{-1} + \Delta U_0)\xi \\ &= V^\top (W_{-1} - \eta_W \chi_0 V (U_{-1} \xi_0)^\top)(U_{-1} \xi - \eta_U \chi_0 W_{-1}^\top V \langle \xi_0, \xi \rangle) \\ &= V^\top W_{-1} U_{-1} \xi - \eta_U \chi_0 \|W_{-1}^\top V\|_2^2 \langle \xi_0, \xi \rangle - \eta_W \chi_0 \|V\|^2 \langle U_{-1} \xi_0, U_{-1} \xi \rangle \\ &\quad + \eta_W \eta_U \chi_0^2 \|V\|^2 \langle \xi_0, \xi \rangle V^\top W_{-1} U_{-1} \xi. \end{aligned}$$

It is not difficult to see that $\eta_U \chi_0 \|W_{-1}^\top V\|_2^2 \langle \xi_0, \xi \rangle$, $\eta_W \chi_0 \|V\|^2 \langle U_{-1} \xi_0, U_{-1} \xi \rangle$, and $\eta_W \eta_U \chi_0^2 \|V\|^2 \langle \xi_0, \xi \rangle$ are all $\Theta(1)$. Unfortunately, here $V^\top W_{-1} U_{-1} \xi = f_{-1}(\xi) = o(1)$ in the infinite-width limit, but if we train one more step, it is easy to see that all four terms of f_0 is $\Theta(1)$. Therefore, pre-training with μP exhibits feature learning.

First step At the first step of fine-tuning, we have $\Delta U_1 = -\eta_U \chi_1 W_0^\top V \xi_1^\top$ and $\Delta W_1 = -\eta_W \chi_1 V (U_0 \xi_1)^\top$. The function can be written as

$$f_1(\xi) = V^\top (W_0 + \Delta W_1)(U_0 + \Delta U_1)\xi,$$

and

$$f_1(\xi) - f_0(\xi) = V'^\top \Delta W_1 U_0 \xi + V^\top W_0 \Delta U_1 \xi + V^\top \Delta W_1 \Delta U_1 \xi. \quad (8)$$

Note that the sum of the first and second terms is exactly $-\chi_1 \mathcal{K}(\xi, \xi_1)$.

Plug in $\Delta W_1 = -\eta_W \chi_1 V (U_0 \xi_1)^\top$ into the first term of eq. (8),

$$V^\top \Delta W_1 U_0 \xi = -\eta_W \chi_1 V^\top V (U_0 \xi_1)^\top U_0 \xi = \Theta(\chi_1),$$

because

$$\begin{aligned} (U_0 \xi_1)^\top U_0 \xi &= (U_{-1} \xi_1 + \Delta U_0 \xi_1)^\top (U_{-1} \xi + \Delta U_0 \xi) \\ &= \langle U_{-1} \xi_1, U_{-1} \xi \rangle - \eta_U \chi_0 \langle \xi_1, \xi_0 \rangle f_{-1}(\xi) - \eta_U \chi_0 \langle \xi, \xi_0 \rangle f_{-1}(\xi_1) + \|\Delta U_0\|^2 \langle \xi_1, \xi \rangle \\ &= \Theta(n). \end{aligned}$$

Plug in $\Delta U_1 = -\eta_U \chi_1 W_0^\top V \xi_1^\top$ into the second term of eq. (8), we have

$$V^\top W_0 \Delta U_1 \xi = -\eta_U \chi_1 V^\top W_0 W_0^\top V \xi_1^\top \xi = \Theta(\chi_1)$$

because

$$\begin{aligned} V^\top W_0 W_0^\top V &= \|(W_{-1} + \Delta W_0)^\top V, (W_{-1} + \Delta W_0)^\top V\|_2^2 \\ &= \|W_{-1}^\top V\|_2^2 + \eta_W^2 \chi_0^2 \|V\|_2^4 \|U_{-1} \xi_0\|_2^2 - 2\eta_W \chi_0 \|V\|_2^2 f_{-1}(\xi_0) = \Theta(1/n). \end{aligned}$$

The third term of eq. (8) equals

$$\eta_U \eta_W \chi_1^2 V^\top V (U_0 \xi_1)^\top W_0^\top V \xi_1^\top \xi = \eta_U \eta_W \chi_1^2 \|V\|^2 \langle \xi_1, \xi \rangle f_0(\xi_1) = \Theta(\chi_1^2),$$

because $f_0(\xi_1) = \Theta(1)$ unlike $f_{-1}(\xi)$ in the ‘‘zero step’’ analysis. Therefore, $\frac{f_1(\xi) - f_0(\xi)}{\chi_1} \rightarrow -\mathcal{K}(\xi, \xi_1)$

⁹ $f_t(\xi)$ is $\Theta(1)$ unless $t = -1$ or there are coincidental cancellations. χ_t is $\Theta(1)$ in pre-training until f memorizes the whole pre-training dataset when $n \rightarrow \infty$.

Second step At the second step of fine-tuning, we have $\Delta U_2 = -\eta_U \chi_1 W_1^\top V \xi_2^\top$, and $\Delta W_2 = -\eta_W \chi_1 V (U_1 \xi_2)^\top$ and

$$f_2(\xi) - f_1(\xi) = V^\top \Delta W_2 U_1 \xi + V^\top W_1 \Delta U_2 \xi + V^\top \Delta W_2 \Delta U_2 \xi. \quad (9)$$

Assuming χ_2 and χ_1 share the same order, then when $n \rightarrow \infty$,

$$\begin{aligned} \frac{f_2(\xi) - f_1(\xi)}{\chi_2} &\rightarrow V^\top \Delta W_2 U_1 \xi / \chi_2 + V^\top W_1 \Delta U_2 \xi / \chi_2 \\ &= -\eta_W V^\top V (U_1 \xi_2)^\top U_1 \xi - \eta_U V^\top W_1 W_1^\top V \xi_2^\top \xi \\ &\rightarrow -\eta_W V^\top V (U_0 \xi_2)^\top U_0 \xi - \eta_U V^\top W_0 W_0^\top V \xi_2^\top \xi \\ &= -\mathcal{K}(\xi, \xi_2). \end{aligned}$$

tth step Same as the second step by noting $\Delta U_t, \Delta W_t$ always have smaller order than ΔU_0 and ΔW_0 .

D.6 STANDARD FINE-TUNING

In standard fine-tuning, V is replaced with a randomly initialized matrix V' . That is, the model at the step t of fine-tuning is $f_t(\xi) = f(\xi; \{U_t^i\}_i, \{W_t^j\}_j, V_t')$. We set $V_0' \sim \mathcal{N}(0, \frac{\sigma^2}{n} I_{n \times d_{out}})$, which has a larger scale than V in μP . In this section, we will prove that this standard fine-tuning has kernel behavior.

Although the infinite width network should exhibit kernel behavior when performing standard FT, we find in practice (Table 5) that the finite-width network does not, suggesting that the infinite width view is not practically useful for discussing standard FT in models of moderate scale. We nevertheless present the proof here and note that it may describe the behavior of wider albeit still finite networks in the future.

coordinate-wise scale	$M = U^i$	$M = W^j$	$M = V$	$M = V'$
M_{-1}	$\Theta(1)$	$\Theta(1/\sqrt{n})$	$\Theta(1/n)$	-
ΔM_0	$\Theta(1)$	$\Theta(1/n)$	$\Theta(1/n)$	$\Theta(1/\sqrt{n})$
ΔM_t	$\Theta(1/\sqrt{n})$	$\Theta(1/n\sqrt{n})$	-	$\Theta(1/n)$
η_M for SGD	$\Theta(1)$	$\Theta(1/n)$	-	$\Theta(1/n)$
η_M for SignGD/Adam	$\Theta(1/\sqrt{n})$	$\Theta(1/n\sqrt{n})$	-	$\Theta(1/n)$

Table 11: Scales for standard fine-tuning w.r.t. n

We still consider a three-layer linear network

$$f(\xi; U, W, V') = V'^\top W U \xi$$

where $V' \in \mathbb{R}^{n \times 1}$ (i.e., $d_{out} = 1$) and we freeze V' during the fine-tuning so it is not trained. Then we have $\nabla_U f = W^\top V' \xi^\top$ and $\nabla_W f = V' (U \xi)^\top$.

First step At the first step of fine-tuning, we have $\Delta U_1 = -\eta_U \chi_1 W_0^\top V' \xi_1^\top$, and $\Delta W_1 = -\eta_W \chi_1 V' (U_0 \xi_1)^\top$. Then the function is now

$$f_1(\xi) = V'^\top (W_0 + \Delta W_1) (U_0 + \Delta U_1) \xi,$$

and

$$f_1(\xi) - f_0(\xi) = V'^\top \Delta W_1 U_0 \xi + V'^\top W_0 \Delta U_1 \xi + V'^\top \Delta W_1 \Delta U_1 \xi. \quad (10)$$

Note the first order and the second order term is exactly $-\chi_1 K(\xi, \xi_1)$.

Plug in $\Delta W_1 = -\eta_W \chi_1 V' (U_0 \xi_1)^\top$ into the first term of eq. (10),

$$V'^\top \Delta W_1 U_0 \xi = -\eta_W \chi_1 V'^\top V' (U_0 \xi_1)^\top U_0 \xi = \Theta(1)$$

since $(U_0 \xi_1)^\top U_0 \xi = \Theta(n)$ ¹⁰.

¹⁰It is clear that $(U_0 \xi_1)^\top U_0 \xi = O(n)$. $(U_0 \xi_1)^\top U_0 \xi = o(n)$ would mean there is some weird correlation.

Plug in $\Delta U_1 = -\eta_U \chi_1 W_0^\top V' \xi_1^\top$ into the second term of eq. (10), we have (assuming $|\xi_1^\top \xi| > 0$)

$$V'^\top W_0 \Delta U_1 \xi = -\eta_U \chi_1 V'^\top W_0 W_0^\top V' \xi_1^\top \xi = \Theta(1)$$

because $V'^\top W_0 W_0^\top V' = \Theta(1)$.¹¹

It is easy to verify that the third term is $O(1/\sqrt{n})$. Therefore, $f_1(\xi) - f_0(\xi)$ converges to its first-order Taylor expansion when $n \rightarrow \infty$.

Second step At the second step of fine-tuning, we have $\Delta U_2 = -\eta_U \chi_1 W_1^\top V' \xi_2^\top$, and $\Delta W_2 = -\eta_W \chi_1 V'(U_1 \xi_2)^\top$ and

$$f_2(\xi) - f_1(\xi) = V'^\top \Delta W_2 U_1 \xi + V'^\top W_1 \Delta U_2 \xi + V'^\top \Delta W_2 \Delta U_2 \xi. \quad (11)$$

We remove all terms of $o(1)$, then

$$\begin{aligned} f_2(\xi) - f_1(\xi) &\approx V'^\top \Delta W_2 U_1 \xi + V'^\top W_1 \Delta U_2 \xi \\ &= -\eta_W \chi_2 V'^\top V'(U_1 \xi_2)^\top U_1 \xi + -\eta_U \chi_2 V'^\top W_1 W_1^\top V' \xi_2^\top \xi \\ &\approx -\eta_W \chi_2 V'^\top V'(U_0 \xi_2)^\top U_0 \xi + -\eta_U \chi_2 V'^\top W_0 W_0^\top V' \xi_2^\top \xi \\ &= -\chi_2 K(\xi, \xi_2). \end{aligned}$$

tth step Same as the second step by noting $\Delta U_t, \Delta W_t$ always have smaller order than ΔU_0 and ΔW_0 .

E SUBSPACE-BASED FINE-TUNING METHODS

We start by restating the Johnson-Lindenstrauss lemma, which preserves inner products under random projection.

Lemma E.1 (Johnson-Lindenstrauss, Johnson (1984)). *Let $u, v \in \mathbb{R}^d$ such that $\|u\| \leq 1$ and $\|v\| \leq 1$. Choose $k = 20 \log N/\epsilon^2$, where N is the number of datapoints. Let $h = \frac{1}{\sqrt{k}} Ax$, where $A \in \mathbb{R}^{k \times d}$ with each entry sampled i.i.d. from $\mathcal{N}(0, 1)$ or $\mathcal{U}(-1, 1)$. Then,*

$$\Pr[|u \cdot v - h(u) \cdot h(v)| \geq \epsilon] \leq \exp(-\epsilon^2 k/4)$$

Lemma E.2 (Norm Preservation (Johnson-Lindenstrauss)). *Let $x \in \mathbb{R}^n$ and assume the entries of $A \in \mathbb{R}^{k \times n}$ are sampled i.i.d. from $\mathcal{N}(0, 1)$. Then,*

$$\Pr \left[(1 - \epsilon) \|x\|^2 \leq \left\| \frac{1}{\sqrt{k}} Ax \right\|^2 \leq (1 + \epsilon) \|x\|^2 \right] \geq 1 - \exp(-(\epsilon^2 - \epsilon^3)k/4)$$

Lemma E.3 (Inner Product Preservation). *Let $u, v \in \mathbb{R}^k$ such that $\|u\|, \|v\| \leq B$. Assume $|\langle u, v \rangle| \geq c \|u\| \|v\|$ (i.e., u and v are not orthogonal). Choose $k = 20 \log N/\epsilon^2$, where N is the number of datapoints. Let $h(x) = \frac{1}{\sqrt{k}} Ax$, where $A \in \mathbb{R}^{k \times n}$ with each entry sampled i.i.d. from $\mathcal{N}(0, 1)$. Then,*

$$\Pr \left[\frac{|\langle u, v \rangle - \langle h(u), h(v) \rangle|}{|\langle u, v \rangle|} \geq \epsilon/c \right] \leq 2 \exp(-(\epsilon^2 - \epsilon^3)k/4)$$

Proof. From the norm preservation in Lemma E.2, we know that with probability at least $1 - 2 \exp(-(\epsilon^2 - \epsilon^3)k/4)$,

$$\begin{aligned} (1 - \epsilon) \|u + v\|^2 &\leq \|h(u + v)\|^2 \leq (1 + \epsilon) \|u + v\|^2 \\ (1 - \epsilon) \|u - v\|^2 &\leq \|h(u - v)\|^2 \leq (1 + \epsilon) \|u - v\|^2 \end{aligned}$$

¹¹It is easy to see that $\mathbb{E}[V'^\top W_0 W_0^\top V'] = \Theta(1)$ and $\text{Var}(V'^\top W_0 W_0^\top V') = \Theta(\|W_0 W_0^\top\|_F^2/n^2)$. By Yang & Hu (2021), $\|W_0 W_0^\top\|_F^2/n^2 = o(1)$.

So, we can write

$$\begin{aligned}
4h(u) \cdot h(v) &= \|h(u+v)\|^2 - \|h(u-v)\|^2 \\
&\geq (1-\epsilon)\|u+v\|^2 - (1+\epsilon)\|u-v\|^2 \\
&= 4u \cdot v - 2\epsilon(\|u\|^2 + \|v\|^2) \\
&\geq 4u \cdot v - 4B^2\epsilon
\end{aligned}$$

This implies $\langle u, v \rangle - \langle h(u), h(v) \rangle \leq B^2\epsilon$. So,

$$\frac{\langle u, v \rangle - \langle h(u), h(v) \rangle}{|\langle u, v \rangle|} \leq \frac{B^2\epsilon}{cB^2} = \epsilon/c$$

The other side of the double-sided bound can be derived analogously. \square

We can now look at LoRA (Hu et al., 2021) for a simple fully connected layer. The construction modifies each layer independently and only acts on fully connected layers, so this is the only part of the kernel that can change when parametrizing updates as in LoRA.

Lemma E.4 (LoRA SGD Kernel). *Let $h = Wx + BAx$ as defined in the paper, where $x \in \mathbb{R}^n$, $W \in \mathbb{R}^{m \times n}$, $B \in \mathbb{R}^{m \times k}$, and $A \in \mathbb{R}^{k \times n}$ with $k \ll n$. B is initialized to 0 and A is initialized with i.i.d. mean-0 Gaussian samples. SGD Training with LoRA (i.e., fixing W and allowing A and B to be updated) yields the kernel $\mathcal{K}_{\text{LoRA}}^{(\text{SGD})}$, whereas full FT with SGD yields the kernel \mathcal{K} :*

$$\mathcal{K}_{\text{LoRA}}^{(\text{SGD})} = dHdH^\top \odot (XA^\top AX^\top) \quad \mathcal{K}^{(\text{SGD})} = dHdH^\top \odot (XX^\top)$$

where $dH \in \mathbb{R}^{N \times m}$ has $dh(x_i)$ in the i th row and $X \in \mathbb{R}^{N \times d}$ has x_i in the i th row.

Proof. We start by noting the well-known fact that $dW = dh \otimes x$, where dh is the gradient to h and \otimes is the cross product. Thus, $K = dHdH^\top \odot (XX^\top)$. In the LoRA setting, $dA = 0$ and $dB = dh \otimes Ax$. Because we are in the kernel setting, $B = 0$ and thus, $dA = 0$, throughout training. So,

$$\mathcal{K}_{\text{LoRA}}(i, j) = \langle dB(i), dB(j) \rangle = \langle dh(i), dh(j) \rangle \langle Ax_i, Ax_j \rangle$$

where $dB(a)$ denotes the gradient to B when given example a . Analogous reasoning yields

$$\mathcal{K}^{(\text{SGD})}(i, j) = \langle dh(i), dh(j) \rangle \langle x_i, x_j \rangle$$

\square

Theorem E.5 ($\mathcal{K}_{\text{LoRA}}^{(\text{SGD})}$ is likely not far from $\mathcal{K}^{(\text{SGD})}$). *Let $\mathcal{K}_{\text{LoRA}}^{(\text{SGD})} \in \mathbb{R}^{N \times N}$ and $\mathcal{K}^{(\text{SGD})} \in \mathbb{R}^{N \times N}$ be defined as in Lemma E.4. Additionally, assume that $|\langle x(\xi), x(\xi') \rangle| \geq c\|x(\xi)\|\|x(\xi')\|$ for some $c > 0$ for all pairs ξ, ξ' in the downstream dataset (i.e., no two gradients are not orthogonal). Then, for any $i, j \in [N]$,*

$$\Pr \left[\frac{|\mathcal{K}_{\text{LoRA}}^{(\text{SGD})}(i, j) - \mathcal{K}^{(\text{SGD})}(i, j)|}{|\mathcal{K}^{(\text{SGD})}(i, j)|} \geq \epsilon/c \right] \leq \exp(-(\epsilon^2 - \epsilon^3)k/4)$$

Proof. Note that

$$\begin{aligned}
\frac{\mathcal{K}_{\text{LoRA}}^{(\text{SGD})}(i, j) - \mathcal{K}^{(\text{SGD})}(i, j)}{|\mathcal{K}^{(\text{SGD})}(i, j)|} &= \frac{\langle dh(i), dh(j) \rangle (\langle Ax_i, Ax_j \rangle - \langle x_i, x_j \rangle)}{\langle dh(i), dh(j) \rangle \langle x_i, x_j \rangle} \\
&= \frac{\langle Ax_i, Ax_j \rangle - \langle x_i, x_j \rangle}{\langle x_i, x_j \rangle}
\end{aligned}$$

The rest of the proof follows from Lemma E.3. \square

The statement for IntrinsicDimension FT (Definition 6.2) can be derived by applying Johnson-Lindenstrauss directly to the gradient vectors.